AD-A114 621 CASE WESTERN RESERVE UNIV CLEVELAND OH DEPT OF MACROM--ETC F/6 11/4
RECENT PROGRESS IN THE STUDIES OF MOLECULAR AND MICROSTRUCTURE --ETC(U)
MAY 82 H ISHIDA N00014-80-C-0533
UNCLASSIFIED TR-4 NL

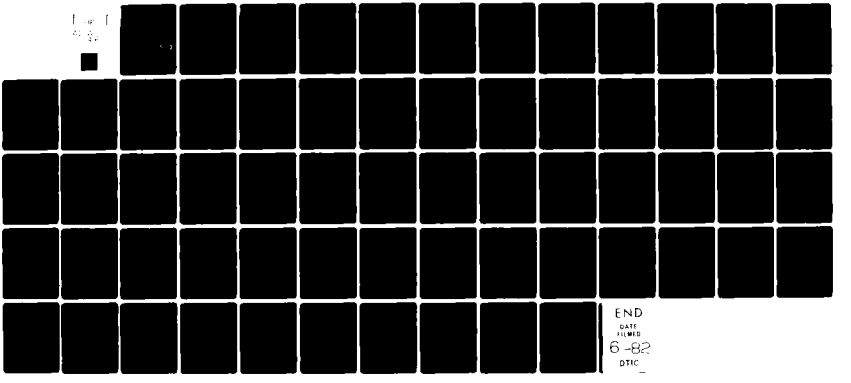

END
DATE FILMED
6-82
DTIC

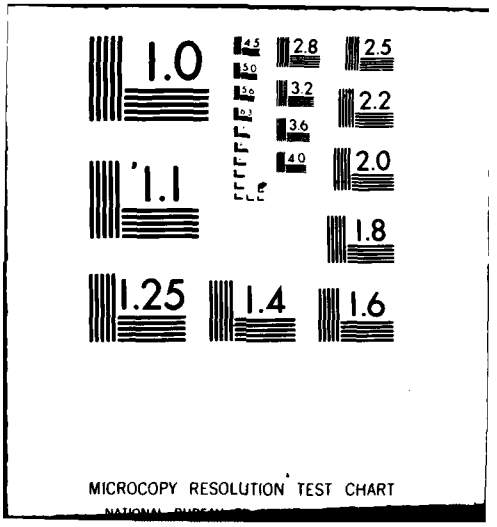
1.0
1.1
1.25
1.4
1.6
1.8
2.0
2.2
2.5
2.8
3.2
3.6
4.0
4.5
5.0
5.6
6.3
7.1
8
MICROCOPY RESOLUTION TEST CHART

SECURITY CLASSIFICATION OF THIS PAGE (When Data Entered)

REPORT DOCUMENTATION PAGE

READ INSTRUCTIONS BEFORE COMPLETING FORM

1. REPORT NUMBER: Technical Report No. 4	2. GOVT ACCESSION NO.: AD-A114 627
3. RECIPIENT'S CATALOG NUMBER	
4. TITLE (and Subtitle): Recent Progress in the Studies of Molecular and Microstructure of Interfaces in Composites, Coatings and Adhesive Joints	5. TYPE OF REPORT & PERIOD COVERED: Technical
	6. PERFORMING ORG. REPORT NUMBER
7. AUTHOR(s): H. Ishida	8. CONTRACT OR GRANT NUMBER(s): N00014-80-C-0533
9. PERFORMING ORGANIZATION NAME AND ADDRESS: Case Western Reserve University, Department of Macromolecular Science, Cleveland, Ohio 44106	10. PROGRAM ELEMENT, PROJECT, TASK AREA & WORK UNIT NUMBERS: NR 356-739
11. CONTROLLING OFFICE NAME AND ADDRESS: Office of Naval Research, Arlington, Virginia 22217	12. REPORT DATE: May 6, 1982
	13. NUMBER OF PAGES
14. MONITORING AGENCY NAME & ADDRESS(if different from Controlling Office)	15. SECURITY CLASS. (of this report): Unclassified
	15a. DECLASSIFICATION/DOWNGRADING SCHEDULE

16. DISTRIBUTION STATEMENT (of this Report)

This document has been approved for public release and sale; its distribution is unlimited.

17. DISTRIBUTION STATEMENT (of the abstract entered in Block 20, if different from Report)

DTIC ELECTE MAY 18 1982 S D E

18. SUPPLEMENTARY NOTES

Submitted to Polymer Composites

19. KEY WORDS (Continue on reverse side if necessary and identify by block number)

Interfaces, Composites, Molecular and Microstructures, The Reinforcement Mechanisms

20. ABSTRACT (Continue on reverse side if necessary and identify by block number)

Recent progress in the studies of molecular and microstructure of interfaces and interphases in composites, coatings and adhesive joints is reviewed. Remarkable progress has been made in elucidating the structure of silane coupling agents and their function with respect to dry and wet strengths of multiphase systems. Aminosilanes attracted major effort in the past. It is now understood that the structure of partially cured hydrolyzate is complicated. When adsorbed from a natural pH solution and dried in

PLEASE TURN OVER

DD FORM 1 JAN 73 1473

SECURITY CLASSIFICATION OF THIS PAGE (When Data Entered)

20. ABSTRACT (continued)

air at room temperature, approximately half of the amine group for amine bicarbonate salt with the CO_2 in air. The rest of the amine groups are either intra- or intermolecularly hydrogen bonded to neighboring silanol groups or free from hydrogen bonding. There exists chemical bonding at the glass/silane or metal/silane interfaces. The surface characteristics, including acidity, topology and homogeneity, influence the structure of the coupling agent. The coupling agent interphase shows a gradient in various properties. Silanes tend to be ordered in the interphase and the degree of organization depends largely on the organofunctionality. The orientation and organization of the silane affect the reinforcement mechanism. There are chemisorbed and physisorbed silanes in the interphase. The coupling agent/matrix interface is a diffuse boundary where intermixing takes place due to penetration of the matrix resin into the chemisorbed silane layers and the migration of the physisorbed silane molecules into the matrix phase. With proper selection of the organofunctionality and the curing conditions, silanes can chemically react with the matrix to form copolymers. The existence of the matrix to form copolymers. The existence of the matrix interphase is now well accepted and the effect of the interphase on the mechanical properties has been studied. It has been recognized that modification of the matrix interphase, such as a coating applied on the fiber using a similar resin as the matrix, has an adverse effect on the mechanical performance. It is noteworthy that attempts to synthesize new coupling agents and to utilize the existing coupling agents more effectively still continue. Based on the molecular understanding, new concepts in the reinforcement mechanism have appeared which have recognized the importance of interpenetrating networks, the structure of silane in the treating solution, and the microheterogeneity of the glass surfaces. The knowledge obtained through the studies of composites can be applied to organic coatings and adhesive joints provided that the geometrical factors are taken into consideration.

RECENT PROGRESS IN THE STUDIES OF MOLECULAR AND MICROSTRUCTURE OF INTERFACES IN COMPOSITES, COATINGS AND ADHESIVE JOINTS

Hatsuo Ishida

Department of Macromolecular Science
Case Western Reserve University
Cleveland, Ohio 44106

ABSTRACT

Recent progress in the studies of molecular and microstructure of interfaces and interphases in composites, coatings and adhesive joints is reviewed. Remarkable progress has been made in elucidating the structure of silane coupling agents and their function with respect to dry and wet strengths of multiphase systems. Aminosilanes attracted major effort in the past. It is now understood that the structure of partially cured hydrolyzate is complicated. When adsorbed from a natural pH solution and dried in air at room temperature, approximately half of the amine group form amine bicarbonate salt with the CO_2 in air. The rest of the amine groups are either intra- and intermolecularly hydrogen bonded to neighboring silanol groups or free from hydrogen bonding. There exists chemical bonding at the glass/silane or metal/silane interfaces. The surface characteristics, including acidity, topology and homogeneity, influence the structure of the coupling agent. The coupling agent interphase shows a gradient in various properties. Silanes tend to be ordered in the interphase and the degree of organization depends largely on the organofunctionality. The orientation and organization of the silane affect the reinforcement mechanism. There are chemisorbed and physisorbed silanes in the interphase. The coupling agent/matrix interface is a diffuse boundary where intermixing takes place due to penetration of the matrix resin into the chemisorbed silane layers and the migration of the physisorbed silane molecules into the matrix phase. With proper selection of the organofunctionality and the curing conditions, silanes can chemically react with the matrix to form copolymers. The existence of the matrix interphase is now well

accepted and the effect of the interphase on the mechanical properties has been studied. It has been recognized that modification of the matrix interphase, such as a coating applied on the fiber using a similar resin as the matrix, has an adverse effect on the mechanical performance. It is noteworthy that attempts to synthesize new coupling agents and to utilize the existing coupling agents more effectively still continue. Based on the molecular understanding, new concepts in the reinforcement mechanism have appeared which have recognized the importance of interpenetrating networks, the structure of silane in the treating solution, and the microheterogeneity of the glass surfaces. The knowledge obtained through the studies of composites can be applied to organic coatings and adhesive joints provided that the geometrical factors are taken into consideration.

INTRODUCTION

Interest in composites ranging from high-performance composites to ordinary particulate-filled composites are rising faster than ever, due to the conservation efforts of raw materials, economic advantages and new requirements for advanced materials. A noteworthy trend has been the effort in developing methods to produce better composites made with particulate fillers which have been historically considered non-reinforcing. Also, the remarkable advancement of modern spectroscopy in the past decade enables one to obtain important molecular information on the glass/matrix interface.

Until the mid 1970's, only preliminary molecular studies including feasibility studies of new spectroscopic techniques had been reported. These studies have been reviewed elsewhere.[1] While feasibility studies using new techniques continue to appear, significant progress has been made in elucidating the structure of interfaces and the function of the coupling agent during the late 1970's and early 1980's. Although voluminous literature exists on the structure and function of various matrices, this subject is beyond the scope of this review article.

The chemical bonding theory dominates many reinforcement theories.[1] However, evidence shows that simple chemical bonding is not sufficient in explaining the interfacial behavior and the reinforcement effect. Attempts will be made to critically review the newer findings and, in some cases, to raise speculative theories based on limited data in order to stimulate further discussion.

To date, the most frequently used techniques in the analysis of interfaces were infrared spectroscopy, including Fourier transform infrared spectroscopy (FT-IR), laser Raman spectroscopy,

secondary ion mass spectrometry (SIMS) with ion scattering spectrometry (ISS), x-ray photoelectron spectroscopy (XPS or ESCA), Auger electron spectroscopy, and gel permeation chromatography (GPC).

STUDIES ON THE STRUCTURE OF COUPLING AGENTS

A. Silanes in Solution

Silane coupling agents have the general form, X_3SiY where X is either a chlorine or an alkoxy group and Y is the organofunctional group. Ordinarily, trialkoxysilane is used because it is easier to handle than the trichlorosilane and the corrosive HCl formed as a by-product of hydrolysis is undesirable. Silanes are applied either from an aqueous or organic solution depending on the type of reinforcements. An aqueous treatment is the usual method for fibrous materials while dry blending is the preferred method for particulate fillers due to the difficulty of drying the aqueous slurry. A hard cake formed after drying requires an additional effort to finely crush the aggregated particles.

In an aqueous solution, a silane is first hydrolyzed to form an organosilanetriol. Hydrolysis is usually complete within one hour; however, the time necessary to completely hydrolyze the silane depends mainly on the organofunctionality, temperature, and the pH of the solution.[2,3] The silanol groups are extremely reactive and condensation reaction proceeds readily even in good solvents such as water at dilute concentrations.[3] The mechanical performance of composites is strongly influenced by the age of the treating solution.[4] The concentration of silane is between 0.01 and 2% by weight in order to ensure predominantly monomeric silane because oligomeric silanes are known to be less effective as coupling agents.[5]

Even in the concentration range where silanetriols dominate the higher oligomers, there is a particular concentration at which an isolated monomer hydrogen bonds forming aggregated monomers. We term this particular concentration as "onset of association." The silanetriol content can be monitored uniquely by laser Raman spectroscopy due to its strong characteristic mode.[3,6,7] The half width at half height of the silanetriol mode shows a sudden increase at 1% by weight for vinyltrimethoxysilane in water indicating the onset of hydrogen bonding between silanols. Note that only the silanetriols are being monitored, and thus, the oligomers are not considered. Above this concentration, the rate of oligomer formation should be much faster, greatly reducing the useful lifetime of the treating solution. The onset of association depends on the organofunctionality and has to be determined individually.

Most neutral silanes predominantly yield silanetriols below one percent by weight when first hydrolyzed. On the contrary, aminofunctional silanes have been believed to yield oligomers even at very dilute concentrations.[8] A wide concentration range of γ-aminopropyltriethoxysilane in water has been studied.[9] When proper hydrolysis conditions were employed, no evidence of unhydrolyzed alkoxy groups was obtained below 30% by weight.[9] Unlike a vinyl functional silane at 10% by weight where monomer predominates,[10] the aminosilane at the same concentration shows major siloxane formation.

An aminosilane in water was studied at a lower concentration range 0.1 - 10% by weight by laser Raman spectroscopy.[11] The characteristic silanetriol line at 712 cm^{-1} was weakly observed in 10% by weight aqueous solution. The intensity of the silanetriol line increases gradually as the concentration of the silane decreases to 1% by weight. Below 1% by weight, the silanetriol content increases rapidly as shown in Figure 1 where the mass adjusted intensity of the silanetriol is plotted as a function of the concentration. It is estimated that the 0.15% by weight solution contains mainly monomers.

At higher concentrations, γ-APS is primarily oligomeric polysiloxanols. The oligomers then form aggregates of submicron size.[11] The hydrodynamic radii determined by the quasielastic laser light scattering technique is shown in Figure 2. These submicron aggregates can be broken into individual oligomers by adding alcohol. It should be noted that these oligomers do not contain an appreciable amount of unhydrolyzed alkoxy groups.

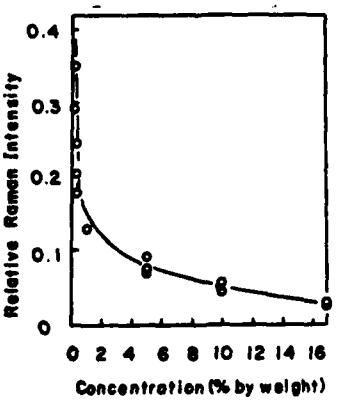

Figure 1. The relative Raman intensity of the aminopropylsilanetriol at 712 cm^{-1} and the ethanol line as an internal standard against the concentration of the solution.

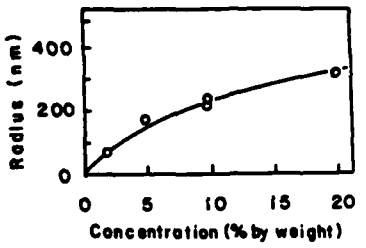

Figure 2. The hydrodynamic radii of γ-APS in water at various concentrations: The γ-APS was vacuum distilled before the use and only freshly hydrolyzed silane was examined.

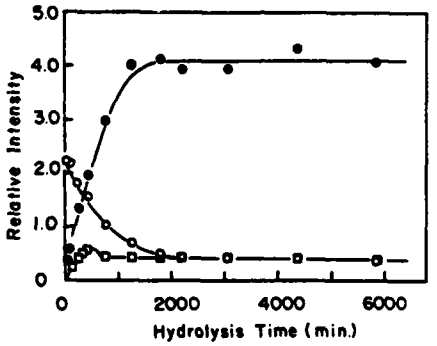

Figure 3. The relative Raman intensity of the γ-APS in water as a function of the hydrolysis time at room temperature: the γ-APS was neutralized with acetic acid prior to the hydrolysis experiment.

○ aminopropyltriethoxysilane

● ethanol

□ aminopropylsilanetriol

On the contrary, when γ-APS is neutralized prior to hydrolysis, the silane forms micelles and hydrolyzes very slowly (Figure 3). Even after 30 hours, a large amount of the alkoxy groups was unhydrolyzed and the level of alkoxy groups remained almost constant. This trend is possibly due to the alkoxy groups that are inside the micelle which are exposed to water.

When more than the stoichiometric amount of acid is added prior to hydrolysis, the catalytic effect of the amine is inhibited and the concentration of silanetriol increases dramatically. The intensity of the Raman line due to the silanetriol is plotted against the amount of acid added in Figure 4.

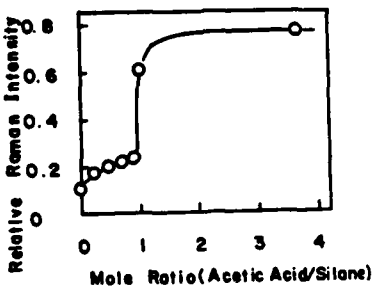

Figure 4. The relative Raman intensity of aminopropylsilanetriol as a function of the mole ratio (acetic acid/silane) prior to hydrolysis at room temperature: the concentration of the aqueous solution was 5% by weight based on the silane. Only freshly hydrolyzed samples were examined. The Raman line due to the propyl chain was used as an internal standard.

B. Silanes on Substrates

1. Factors Affecting the Silane Interphase

The factors that influence the structure of the coupling agent layers and subsequently the mechanical and physical properties of composites are the structure of the silane in the treating solution, the organofunctionality of the silane, the drying conditions, the topology of the reinforcement, and the chemical composition of the surface. Thus, it is essential to study the relationship between these factors and the structure of the silane interface. There are many variables that characterize the structure of the silane interphase. These include the silane up-take, the uniformity of the thickness of the silane layers, the orientation and organization of the silane molecules, degree of siloxane formation, the molecular weight and its distribution, the degree of available organofunctionality for copolymerization with the matrix, the interaction between the surface and the organofunctionality, the structural gradient, and the amount of the physisorbed silanes on the outermost layers. The influence of these factors is complex and very few direct correlations with the mechanical performance of composites have been reported.

2. Aminosilanes

An extensive effort has been made in the past several years to elucidate the structure of aminosilanes. Unlike other neutral silanes, aminosilanes show anomalous behavior in solution and on substrates. For example, even high concentrations of aqueous solutions show remarkable stability for long periods of

time without causing precipitation.[12] Also, a 50% by weight alcohol solution of an aminosilane gels immediately upon the addition of 2 moles of water (based on the silane) but becomes liquid again after standing overnight.[13] The contact angle of the aminosilane treated glass does not exhibit the angle expected from the amine groups but yields the value of 35 dynes/cm which represents a nonpolar surface.[14]

Modern spectroscopic methods have been applied to investigate the structure of aminosilanes. Early studies by Bascom,[15] Kaas and Kardos,[16] and Nichols et al.[17] are reviewed elsewhere.[1] Emphasis in these studies as well as later studies was focused on the structure of the amine group of the silane molecule. Anderson et al.[18] reported that the N_{1s} peak in their ESCA spectra showed a doublet at 399.0 and 400.5 eV for a hydrolyzed γ-aminopropyltriethoxysilane (γ-APS) on a silicon wafer. The hydrolyzate of γ-APS was exposed to hexafluoroisopropanol, a Lewis acid analogue of the plasma polymerized polytetrafluoroethylene of their interest, and the subsequent peak shifts were observed by ESCA. The exposed sample showed spectral changes in all elements, i.e., Si_{2p}, C_{1s}, N_{1s} and F_{1s} peaks, instead of a preferential change in the N_{1s} peak as expected. They concluded that the amine was in the protonated form otherwise the amine would be highly sensitive to the presence of a Lewis acid. From this result, they concluded that the γ-APS layers contain appreciable amounts of the silanol groups. It should be noted that this conclusion is valid when silanol only is known to be the proton donor.

The classic paper by Plueddemann[2] which hypothesized either an intramolecular five-membered or six-membered ring for the aminosilane molecule strongly influenced later studies. An infrared reflection-absorption study by Boerio and Geivenkamp[19] of γ-APS on an iron substrate showed that a strong infrared band appeared at 1575 cm^{-1} when γ-APS was adsorbed onto an iron coupon from a 1% by weight aqueous solution (Figure 5). The band at

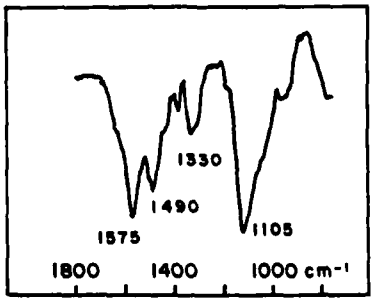

Figure 5. Infrared reflection-absorption spectrum of γ-APS on an iron mirror which was treated with a 1% by weight solution and dried at room temperature. Two reflections at 78°.

1575 cm^{-1} was assigned to the amine group coordinated to the silicon atom. However, no proper model compound for an amine group pentacoordinated to a silicon atom is known. The closest model compound for this is a series of silatrane molecules where three alkoxy groups are attached to the nitrogen atom. The nitrogen atom is then pentacoordinated to the silicon atom, which creates strained loops of three alkoxy groups.[20-22] In this structure, the nitrogen is a tertiary amine and the nitrogen is forced to be close to the silicon atom resulting in the pentacoordination. The amine group is known to pentacoordinate to the silicon atom when a strained loop is attached to the silicon. Unlike silatranes, the hydrolyzate of γ-APS does not have a strong driving force to form a pentacoordinated structure nor does the infrared spectrum of unhydrolyzed γ-APS show any signs of a specially coordinated amine.[9] Instead, several analogues of γ-APS all show a doublet near 1610 cm^{-1} in their pure form. This indicates the presence of hydrogen bonded amines acting as proton donors and acceptors.[9]

When the γ-APS on an iron coupon was washed with water, the strong infrared band at 1575 cm^{-1} disappeared and the band at 1510 cm^{-1} became the strongest band in the spectrum. The intensity of all bands decreased due to the decreased thickness (Figure 6). The 1510 cm^{-1} band was then assigned to the $-NH_3^+$ group of a cyclic zwitterion.[19] Judging from the sharpness of the observed band at 1510 cm^{-1}, it seems rather unlikely that it could be the $-NH_3^+$ of the zwitterion which has a large range of structural and orientational freedom resulting in a broad peak.

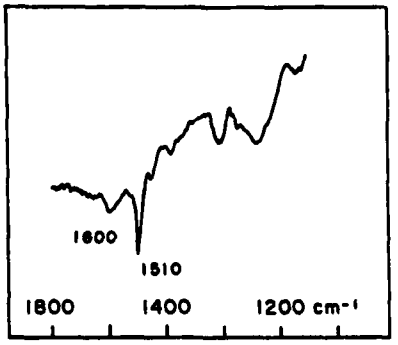

Figure 6. Infrared reflection-absorption spectrum of γ-APS on iron. The same sample as in Figure 5 except that the silane was washed with water for 15 minutes at room temperature. Two reflections at 78°. The intensities of the major bands are approximately 10% of the spectrum in Figure 5.

The significance of Boerio et al.'s paper lies in their findings of a structural gradient as a function of thickness of the silane layers and demonstration of the usefulness of the infrared reflection-absorption spectroscopy initially developed by Francis et al.[23] and Greenler.[24]

The preliminary work reported by Diaz et al.[25] using inelastic electron tunneling spectroscopy showed a similar feature which was reported by Boerio et al. using infrared spectroscopy for γ-APS on iron which was washed with water.[19] Aluminum oxide was used as the substrate and a monolayer quantity of γ-APS was adsorbed from unhydrous solvents. The selection rules for the inelastic electron tunneling spectrum are unique in that both the infrared and Raman active modes can be observed in comparable intensities. Also it shows an orientation effect which yields a high intensity band when the vibration is normal to the metal surface. It is likely that Boerio et al.[19] and Diaz et al.[25] observed the γ-APS whose amine group was hydrogen bonded to the surface hydroxyl groups of the metal.

The hydrogen bonded amine along with the protonated amine were also reported by Moses et al.[26] using ESCA with a SnO_2 electrode as a substrate. The SnO_2 electrode treated with a dilute aqueous solution of γ-APS showed a doublet in the N_{1s} peak at 400.3 and 401.9 eV, which was slightly different in their absolute energies from those reported by Anderson et al.[18] but were almost identical in the separation energy of the two peaks. The γ-APS on the electrode was exposed to 0.05M HCl aqueous solution. As shown in Figure 7, the 401.9 eV peak increased in intensity compared to the sample exposed to a pH 10 aqueous base indicating that the peak at 401.9 eV is due to the protonated amine and that its proportion increases by forming the amine hydrochloride salt. Moses et al. also studied the relative intensity of the protonated amine versus free amine as a function of the pH of the environmental solution as shown in Figure 8 for β-aminoethyl-γ-aminopropyltriethoxysilane(en-silane) and observed discontinuities near the pK_a values (6.85 and 9.93) of free ethylenediamine. This demonstrates that the aminosilane functions on a substrate similar in basicity to that of the corresponding amines. It should be noted, however, that the reactivity may be altered. Based on their results, they postulated an intramolecularly interacting amine with the silanol groups either in a protonated form or an unprotonated form, though they did consider the hydrogen bonding with the substrate as reported by Lee,[27] Plueddemann,[28] and Weetall and Hersh.[29]

An application of Fourier transform total internal reflection spectroscopy (ATR) using crystalline Al_2O_3 was reported by Sung et al.[30] Using a substrate of interest, which is transparent to

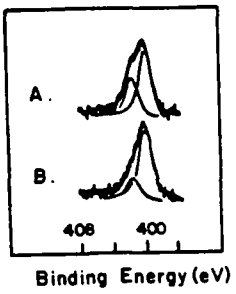

Figure 7. N_{1s}ESCA spectra of SnO_2 electrode treated with γ-APS. The electrode was exposed to A., 0.05 M HCl and B., pH = 10 aqueous base.

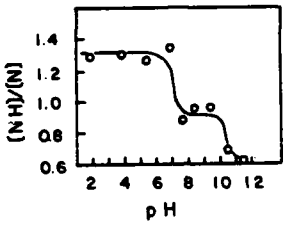

Figure 8. Ratio of the ESCA peak heights of the protonated amine and unprotonated amine. Diaminofunctional silane (en-silane) was used to treat a SnO_2 electrode. A different sample was used for each data point.

a wide range of infrared radiation, as an ATR plate is useful because it has an excellent optical contact at the ATR plate/surface species interface. This approach was used effectively by Bershtein et al.[31,32] for the study of the hydrolysis of SiO_2 surface using a SiO_2 plate as an ATR plate. Sung et al.[30] reported the relative intensity of the amine band near 1590 cm^{-1} of γ-APS which was mass adjusted by the CH stretching mode at 2940 cm^{-1}. Since the propyl group of the silane as well as the alkoxy group heavily overlap around 2940 cm^{-1} the intensity of this band decreased as the hydrolysis proceeded. The relative intensity of the amine group decreased as the thickness increased. They used this ratio to study the extent of hydrolysis and cross-linking of the silane layers. However, since the intensity of the amine band around 1590 cm^{-1} varied dramatically depending on the strength of the hydrogen bonding and the salt formation described in a later section, the validity of the ratio used is questionable. Furthermore, the complex overlapping of the CH_2 vibration of the propyl chain and the ethoxy group makes intensity

measurements inaccurate. Therefore, the ratio does not represent the extent of hydrolysis nor the degree of cross-linking, although these are the factors which influence the ratio.

Also reported by Sung et al.[30] was a partially hydrolyzed γ-APS when the concentration range was between 1 - 3% by weight. As stated earlier, if γ-APS is properly hydrolyzed, namely using neutral water and hydrolysis time of more than 15 minutes with freshly distilled silanes, there is no evidence of a partially hydrolyzed silane in less than 30% by weight solutions,[9] since the amine group selfcatalyzes the hydrolysis. Owing to the very high sensitivity of the structural variation observed for γ-APS, it is essential to control the hydrolysis conditions and to have reproducible drying conditions.

Chiang et al.[33] hypothesized an intramolecular hydrogen bonded structure I,

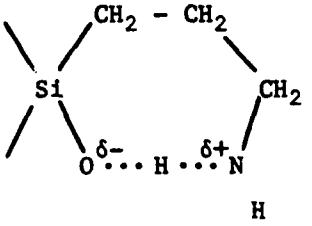

(I)

along with the hydrogen bonding with the surface silanols. The hydrogen bonded structure was subsequently supported by Boerio et al.[34] from the study of γ-APS on iron and aluminum substrates. They assigned the strong bands near 1550 and 1470 cm^{-1} to the hydrogen bonded amine group. In addition, the band near 1600 cm^{-1} was assigned to the accidental degenerate modes of the NH_2 deformation of the free amine and the protonated amine associated with an intramolecular zwitterion or an amine salt from the solution. However, little evidence supporting these assignments was reported.

Boerio and others[34] further studied propylamine adsorbed on an iron surface. Only one band was observed between 1600 and 1200 cm^{-1}, at 1500 cm^{-1}, which was assigned to the $-NH_3^+$ symmetric bending mode (Figure 9). If the propylamine is protonated and oriented normal to the surface, the $-NH_3^+$ symmetric bending mode should appear as a strong band. This band at 1500 cm^{-1} is analogous to the band at 1505 cm^{-1} observed earlier for a very thin γ-APS on iron by Boerio et al.,[19] indicating that they observed the direct interaction between the metal surface and the coupling agent.

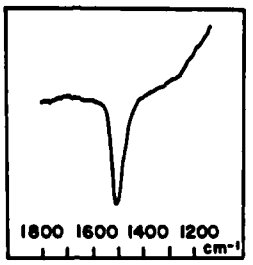

Figure 9. Infrared reflection spectrum of propylamine adsorbed on an iron mirror. The mirror was immersed in 0.5% aqueous solution of n-propylamine at pH = 12.4 for 30 minutes and dried. Two reflections at 78°.

Evidence of a specially interacting amine was also observed by Sung et al.[35] using ESCA. Similar to the other ESCA results for γ-APS on substrates,[18,26] they also observed a doublet on the N_{1s} peak at 399 and 401.3 eV. The free amine peak at 399. eV disappeared after washing with water followed by an acetone wash. The observation of the protonated amine at the substrate/silane interface is consistent with Boerio et al.'s observation as described above.[34] ESCA was also used by Boerio et al.[34] in their study of γ-APS on iron and a doublet at 399.6 and 401.5 eV was reported.

Ishida et al.[9] studied γ-APS and its analogues as aqueous solutions as well as partially cured solids using Fourier transform infrared and laser Raman spectroscopy. Unlike previous researchers, they focused their attention on the silanol part of the molecule. The partially cured hydrolyzate of γ-APS shows a weak peak at 930 cm^{-1} which is near the SiO stretching mode of the silanol. However, except for aminosilanes, no other neutral silane shows a band above 910 cm^{-1} for monosilanol.[36] Table I lists the SiO antisymmetric and symmetric stretching modes of various organotrialkoxysilanes and their hydrolyzates. Gamma-aminopropyltrisilanolate, $NH_2(CH_2)_3SiO_3^{3-}$, was prepared in a KOH aqueous solution. The Raman spectrum confirmed predominant formation of the monomeric organotrisilanolate. The FT-IR difference spectrum of the same solution showed strong bands at 970 cm^{-1} and 930 cm^{-1} as the antisymmetric SiO_3^{3-} modes and the absence of the SiOSi groups. Consequently, the band at 930 cm^{-1} was considered to be too low for the frequency of the SiO^- group and, instead, assigned to the strongly hydrogen bonded SiOH groups. It was concluded that intramolecular zwitterions do not exist based on the above reason and heat treatment experiments. They also estimated that nearly half of the amines are either free from hydrogen bonding or only weakly hydrogen bonded.

Controversy over the strong infrared bands near 1630, 1570, and 1470 cm^{-1} still continues. Boerio et al.[37] hypothesized that these bands are due to either the hydrogen bonding as shown in structure (I) or to an amine bicarbonate salt. They stated that the aliphatic amine salt showed a similar infrared spectrum compared to the spectrum of γ-APS deposited on a metal surface from a natural pH solution.

Very recently, Naviroj et al.[38] confirmed that carbon dioxide in air forms an amine bicarbonate salt when γ-APS is deposited on a substrate at natural pH. The infrared bands around 1630 and 1332 cm^{-1} are compared to sodium bicarbonate and assigned to the vibrational modes due to the bicarbonate ion HCO_3^-.[39] The strong bands at 1570 and 1470 cm^{-1} are due to the amine counterpart and assigned to the symmetric and antisymmetric vibration of the $-NH_3^+$ ion. When the hydrolyzate of γ-APS from natural pH was dried under a nitrogen atmosphere, the controversial strong bands all diminished and a singlet remained at 1600 cm^{-1}, which was assigned to the NH_2 group. FT-IR analysis of an air-dried, heat treated γ-APS showed spectroscopic evidence of evaporated CO_2. Chemical analysis also confirmed that CO_2 was generated as a result of the decomposition of amine bicarbonate salt.[40] Figure 10 compares the γ-APS dried in air, CO_2, and N_2 atmosphere.[38] Note that the dramatic intensification of the bands in the range 1700 - 1200 cm^{-1} is due to the salt formation.

Confirmation of the amine bicarbonate salt formation is consistent with the former observation that the SiO^-, which would have resulted from the zwitterion formation, is unlikely to exist.[9] Also consistent with the above findings is the observation of the

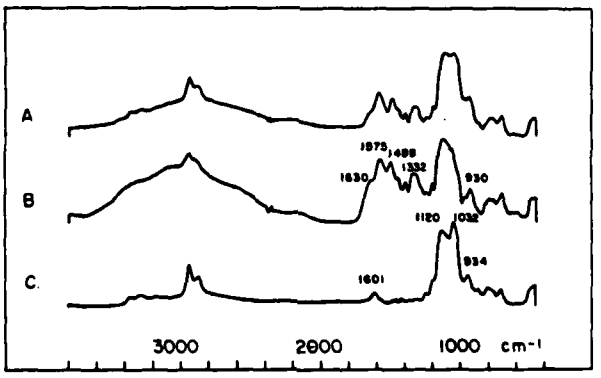

Figure 10. FT-IR absorbance spectra of the hydrolyzate of γ-APS dried in A., air; B., CO_2, and C., N_2 atmosphere at room temperature.

Table I. The SiO Antisymmetric and Symmetric Stretching Frequencies of Organotrialkoxysilanes, Organosilanetriols, and Organotrisilanolates.

No.	Name	Chemical Formula	$RSi(OR')_3$		$RSi(OH)_3$	
			IR	Raman	IR	Raman
1.	Triethoxysilane	$HSi(OEt)_3$	701	698		
2.	Methyltrimethoxysilane	$CH_3Si(OMe)_3$	627	626		692
3.	Methyltriethoxysilane	$CH_3Si(OEt)_3$	645	643	927,855	
4.	Methyltri-n-propoxysilane	$CH_3Si(O\text{-}n\text{-}Pr)_3$	656	650		
5.	Ethyltrimethoxysilane	$CH_3CH_2Si(OMe)_3$	613	610		
6.	Ethyltriethoxysilane	$CH_3CH_2Si(OEt)_3$	633	635	910,848	669
7.	n-Propyltrimethoxysilane	$CH_3(CH_2)_2Si(OMe)_3$	639	640,608	915,844	704,653
8.	n-Propyltriethoxysilane	$CH_3(CH_2)_2Si(OEt)_3$	650,628	647,626		
9.	n-Propyltri-n-propoxysilane	$CH_3(CH_2)_2Si(O\text{-}n\text{-}Pr)_3$	652,637	658,640		
10.	n-Propyltri-n-buthoxysilane	$CH_3(CH_2)_2Si(O\text{-}n\text{-}Bu)_3$	653,637	658,640		
11.	n-Buthyltrimethoxysilane	$CH_3(CH_2)_3Si(OMe)_3$	645,610	639,609		
12.	Vinyltrimethoxysilane	$CH_2{=}CHSi(OMe)_3$	622	622	927,848	678
13.	Vinyltriethoxysilane	$CH_2{=}CHSi(OEt)_3$	633	635	927,848	678
14.	N-β-aminoethyl-γ-aminopropyl-trimethoxysilane	$NH_2(CH_2)_2NH(CH_2)_3Si(OMe)_3$	647,613			
15.	γ-Aminopropyltrimethoxysilane	$NH_2(CH_2)_3Si(OMe)_3$	645,615	640,612		
16.	γ-Aminopropyltriethoxysilane	$NH_2(CH_2)_3Si(OEt)_3$		650,619		
17.	Chloromethyltrimethoxysilane	$ClCH_2Si(OMe)_3$	610	609		
18.	γ-Chloropropyltrimethoxysilane	$Cl(CH_2)_3Si(OMe)_3$	640,612	639,611	923,840	689,643
19.	Cyclohexyltrimethoxysilane	 $Si(OMe)_3$	660	660		723
20.	β-Cyanoethyltriethoxysilane	$CN(CH_2)_2Si(OEt)_3$	627	627,658		
21.	β-(3,4-Epoxycyclohexyl)ethyl-trimethyloxysilane	 $(CH_2)_2Si(OMe)_3$	643,612	640,609	920,851	718,652
22.	γ-Glycidoxypropyltrimethoxy-silane	 $CH_2{-}CHCH_2O(CH_2)_3Si(OMe)_3$	644,612	642,611	923,850	715,655

23. 3-Mercaptopropyltrimethoxysilane	$SH(CH_2)_3Si(OMe)_3$	640,610	639,611		
24. 3-Methacryloxypropyltrimethoxysilane	$CH_2{=}C(CH_3)-CO(CH_2)_3Si(OMe)_3$				
25. Phenyltrimethoxysilane	 $Si(OMe)_3$	645,613 656	643,611 655	922,853 930,832	714,657 696,693
26. Phenyltriethoxysilane	 $Si(OEt)_3$	660	664		
27. N-(Trimethoxysilylpropyl)-imidazole	 $N(CH_2)_3Si(OMe)_3$	631,606			
28. 3-Aminopropyltrisilanolate	$NH_2(CH_2)_3SiO_3^{3-}$ in KOH sol.			972,915	705,652
29. Vinyltrisilanolate	$CH_2{=}CHSiO_3^{3-}$ in KOH sol.			956,907	664

Abbreviations:

Me = CH_3

Et = CH_2CH_3

n-Pr = $(CH_2)_2CH_3$

n-Bu = $(CH_2)_3CH_3$

characteristic features of an amine salt in the 3000 - 2000 cm^{-1} region. An immediate and important consequence of the amine bicarbonate salt is the formation of a linear chain salt. Structural influence on the siloxane network could be important since an intramolecular cyclic structure would restrict the reactivity of the silanol involved while the linear chain salt would not significantly affect its reactivity. It should be noted, however, that not all amines form the bicarbonate salt. A preliminary result showed that approximately half of the amines are either free or weakly hydrogen bonded as stated above.[40] Therefore, it is still possible that some amines may form intramolecular hydrogen bonded structures while the others may be intermolecularly hydrogen bonded. Thus, the complexity of the partially cured γ-APS is now well documented. It is this complexity that leads many researchers to various hypotheses.

3. The Coupling Agent Interphase

In addition to the extensive efforts in elucidating the structure of aminosilanes, other silanes have also been investigated. While the specific nature of silanes containing various organofunctionalities have been highlighted, attempts have been made to generalize these observations. The major silanes studied include γ-methacryloxypropyltrimethoxysilane (γ-MPS), γ-glycidoxypropyltrimethoxysilane (γ-GPS), vinyltrimethoxysilane (VS) and cyclohexyltrimethoxysilane (CS).

Ishida and Koenig[41] studied the chemical reaction between a high-surface-area silica and a vinyl functional silane using Fourier transform infrared spectroscopy (FT-IR). The digital subtraction technique was used to generate the difference spectrum of the VS on the silica surface. Immediately following the silane deposition and drying with nitrogen, the characteristic silanetriol band at 674 cm^{-1} was observed indicating that the initial silane adsorption could be a hydrogen bonding through the strongly adsorbed water on the silica surface. Upon drying, the silanol band of VS weakened indicating siloxane formation. Quantitative measurement of the number of silanols per repeat unit of the polysiloxanol resulted in 0.07 for a well dried sample. Since approximately a monolayer coverage was used and the indication of a random and uniform adsorption was observed, the above value indicates covalent bond formation at the silica/silane interface. Further qualitative evidence shown in Figure 11 was obtained using oligomeric siloxanol which showed the disappearance of the surface silanol at 970 cm^{-1} and the silanol of the silane at 894 cm^{-1} and the appearance of the siloxane bands in the 1200 - 1000 cm^{-1} range. The newly arisen siloxane bands differed both from the pure silica or the polyvinylsilsesquioxane in frequency indicating that the reaction product is unique to the interface.

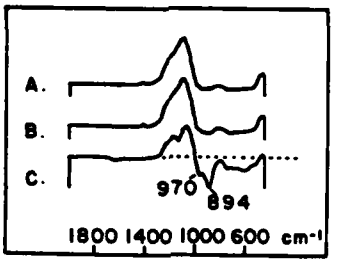

Figure 11. FT-IR absorbance and difference spectra: A., a fumed silica treated with 1% by weight polyvinylsiloxanol in isopropanol before the heat treatment at 150°C for 30 minutes; B., the same sample as A. but after the heat treatment; C., the difference spectrum (B. - A.). The fumed silica was heat treated at 600°C overnight prior to the silane treatment. The KBr pellet method was used for obtaining the spectra.

The study by Ishida et al.[42] using E-glass fiber as a substrate reconfirmed the previous observations of multilayer formation on smooth surfaces as reported by Schrader et al.[43] and Johannson et al.[44] using radioisotope-labeled coupling agents. Ishida et al.[42] studied the condensation reaction of the silanols with and without the substrates. They found that the silanol on the surface of E-glass fiber condensed faster than the silanol without the substrate. Since the silane was too thick to consider the surface catalytic effect on the condensation, they postulated an ordered structure in the coupling agent interphase.

The silane up-take studied as a function of the concentration of the treating solution showed a break point near 1% by weight (Figure 12) whose concentration agrees with the previously discussed onset concentration of association. Similar breakpoints on the silane up-take vs concentration curves have been observed for γ-MPS and γ-APS at 0.4% and 0.15% by weight, respectively. These concentrations are the onset concentrations of the corresponding silanes.[45,11]

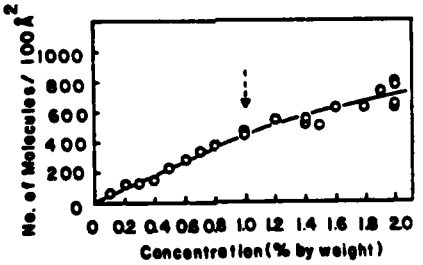

Figure 12. Up-take of a vinyl functional silane against the concentration of silane treating solutions.

Further study of the organization of the silane layers on E-glass fiber was made using VS.[46] The silane deposited from the solution with various concentrations was used to study the previously observed faster rate of silanol condensation on the glass fiber surface. The mass adjusted infrared intensity of the silanol band showed almost complete condensation when adsorbed from the solution at concentrations less than 1% by weight and dried at room temperature for 135 hours (Figure 13). However, above 1% by weight, the residual silanols were observed for the same drying conditions. Again, the transition of the residual silanol appearance coincided with the onset concentration of association.

In order to test the possible catalytic effect of the surface, the silane was adsorbed from the same solution at 4% by weight but the glass fibers were rinsed immediately after the adsorption with water at various strengths. This allowed the thickness of the silane layers to be varied while the organization of the molecule was maintained. The amount of residual silanol is plotted against the silane up-take as shown in Figure 14. Even the thickness range corresponding to less than 1% by weight solution in the previous concentration experiment showed residual silanols indicating that the surface catalytic effect is not a major cause of the observation in Figure 13. Rather the organization of the silane molecules upon adsorption influence the condensation reaction. At the very thin layers, however, some indication of surface catalytic effect is evident.

The molecular organization of the coupling agent interphase is a direct consequence of the surface topology.[46] It is known that the surface of glass fibers is smooth with respect to the size of nitrogen molecules while ground fibers have a roughened surface. The surface chemical composition of these two glasses are similar, yet, the smooth glass fiber gives a multilayer adsorption whereby the roughened surface adsorbs nearly a monolayer, or very thin layers. It was thought that the preferential orientation of the molecular axis of silane can support the subsequent layers when the silane is on a smooth surface. On the other hand, a random orientation on the roughened surface interferes with the formation of an organized layer.

An extreme case of ordered layers was observed when cyclohexyltrimethoxysilane (CS) was adsorbed from an aqueous solution onto E-glass fiber. Cyclohexylsilanetriol is one of the very few silanes that can be crystallized without detectable silanol condensation. The FT-IR spectrum of cyclohexylsilanetriol crystals was very similar to the difference spectrum of the CS adsorbed on E-glass fibers suggesting that a crystalline-like structure is formed on the surface. Similar tendencies exist with many silanes but the degree of order depends mainly on the rigidity of the

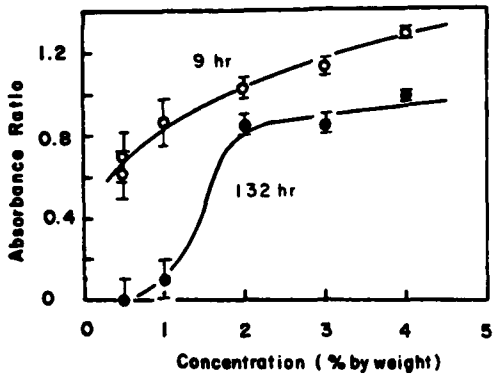

Figure 13. Amount of the residual silanol of a vinyl functional silane on E-glass fibers as a function of the concentration of silane treating solutions. The silane-treated glass fibers were dried at room temperature for 9 and 135 hours, respectively. The infrared absorbance ratios of the silanol band against the vinyl band were measured to represent the mass-adjusted residual silanols.

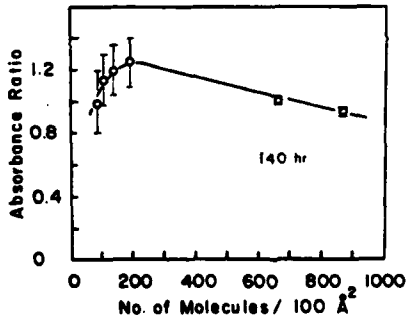

Figure 14. Amount of the residual silanol of VS on E-glass fibers with various silane up-takes. Only one silane solution was used to prepare all samples but rinsed with water with varying strength in order to produce thickness variation of the silane interphase. Approximately 250 molecules/100Å^2 corresponds to the transition seen in Figure 13.

organofunctionality. Thus, the tendency of ordered layer formation decreases in the order , —> CH_2═ CH—, CH_3CH_2—, CH_3—,>

which is in accord with the stability of silanetriol.

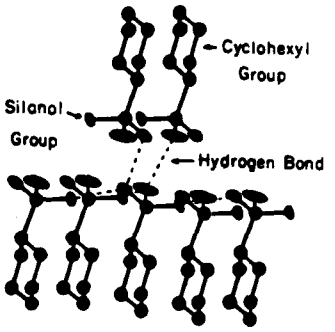

Figure 15. X-ray crystal structure of a single crystal of cyclohexylsilanetriol.

The ordered layers are likely to have head-to-head arrangement. Indirect support comes from the fact that, according to the x-ray crystallographic study of a single crystal of cyclohexylsilanetriol,[47] the molecules arrange themselves in a head-to-head position as shown in Figure 15. The driving force for this structure is obviously hydrogen bonding but, interestingly, it is not a simple linear hydrogen bonding which is a common structure of many known hydrogen bonded systems. Instead, the silanol forms a bifurcated hydrogen bonding in which a proton is shared statistically by two adjacent oxygens, simultaneously. Moreover, a sheet of cyclohexylsilanetriol is hydrogen bonded to the neighboring sheet of the silanetriols, thus bilayers act as a unit. This is, of course, an extreme case of ordered silane layers and actual industrially useful silanes do not show such a high degree of order. Nonetheless, it should be recognized that all silanes show this tendency to some extent. The degree of order in the silane interphase may be an important factor for an interpenetrating network formation. This idea is presented in a later section and is proposed as one of the reinforcement mechanisms in addition to the chemical bonding theory.

There are reports which state that a gradient in the coupling agent interphase exists. An early study by Schrader, et al.[43] using radioisotope-labeled silane has been reviewed.[1] They reported an increased tenacity to desorption by water extraction as the thickness of the silane interphase decreases.

DiBenedetto and Scola[48] using ISS and SIMS showed that the γ-APS interphase on S-glass fiber has three different regions with respect to the signal intensity of the SIMS spectrum during the depth profile study by the ion sputtering technique. The strongest

signal was obtained in the outermost layers. They related the signal intensity with the mobility of the polysiloxane and concluded that the molecular weight is highest in the outermost layers, the lowest in the middle layers and again became higher near the glass surface. The observation of the high-molecular-weight outermost layers seems to contradict the desorption characteristics of γ-APS in water reported by Schrader et al.[43] and Johannson et al.,[44] where the initial desorption took place very rapidly. The reason for this discrepancy is not known at the present time. However, since the SIMS instrument, as well as the ESCA and Auger, utilizes ultra-high vacuum during the experiment, the previously stated amine bicarbonate salt of γ-APS may have decomposed and subsequent structural changes may have caused the difference.

Hydrothermal degradation of composite interfaces has been one of the most discussed subjects in the past based on the indirect observations. The degradation mechanisms are of great interest. Qualitative observations of hydrolysis of the polysiloxane networks have been reported.[49] Figure 16 shows FT-IR difference spectra of VS on E-glass fiber before and after the immersion test in water for about 1500 hours at 80°C. The band appearing at 890 cm^{-1}, which is absent in the spectrum before the hydrothermal treatment, is attributed to the silanol as a product of the hydrolysis.

Desorption characterics of various silanes were also studied by Ishida and Koenig.[50] Remarkable variation in the desorption

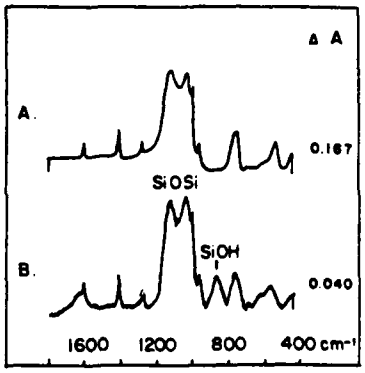

Figure 16. FT-IR difference spectra of VS on E-glass fibers before (A.) and after (B.) the hydrothermal treatment at 80°C for 1500 hours. A new band appeared around 890 cm^{-1} after the treatment due to the silanol groups as a result of the hydrolysis of the siloxane groups.

characteristics have been observed for γ-MPS, VS and CS as shown in Figures 17, 18, and 19, respectively. The desorption curve of

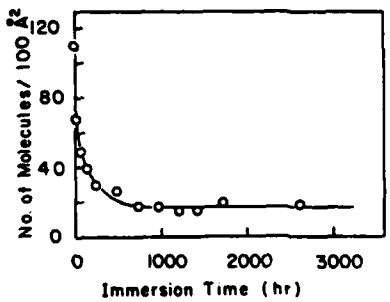

Figure 17. Desorption curve of γ-MPS on E-glass fibers against the immersion time in water at 80°C.

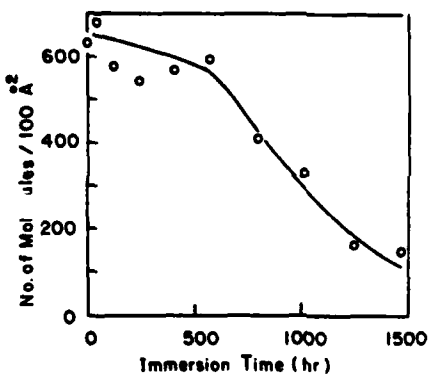

Figure 18. Desorption curve of VS on E-glass fibers against the immersion time in water at 80°C.

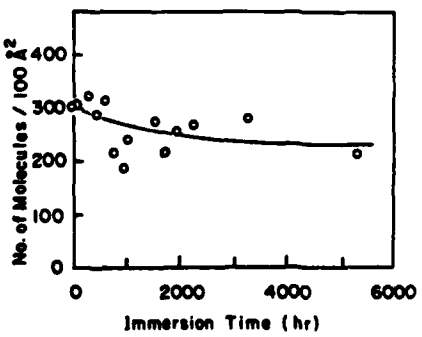

Figure 19. Desorption curve of CS on E-glass fibers against the immersion time in water at 80°C.

γ-MPS is similar to γ-APS where the initial desorption is the fastest followed by an exponential decay in the desorption rate. A specific feature of γ-MPS is that, near the glass surface at several monolayers of thickness, an extremely resistant layer to desorption exists due to the formation or organic chains by surface induced homopolymerization of γ-MPS. Reduced solubility by extended organic chain length may be attributed to this tenacity. This is substantiated by the observation that no desorption took place when the silane interphase was copolymerized with a matrix. Therefore, the difficulty for desorption near the glass surface reported by Schrader et al. is fundamentally different in nature[43] since they attributed the cause to be due to the extensive cross-linking formation at the glass/silane interface through the siloxane linkages.

VS showed an initial threshold period followed by a relatively quick desorption. It was thought that since the relatively high degree of order in the silane interphase would lead to an extensive open structure rather than a cyclic structure, the silane interphase needed to be hydrolyzed until the solubility of the oligomers became sufficient to dissolve them in water. However, continuous hydrolysis has been observed during the threshold period.

4. The Substrates/Coupling Agent Interface

A new technique which is particularly suitable for the mobility study of silane molecules on glass surfaces is on the horizon. High-resolution solid-state NMR with magic angle spinning and cross polarization capability has recently become available.[51-55] Preliminary attempts have been made by Chiang et al.,[56] Leyden et al.,[57] Hayes et al.,[58] and Ritchey and Koenig[59] using a high-surface-area silica as a substrate and well resolved solid-state ^{13}C-NMR spectra were obtained. An example is shown in Figure 20. Although no data has yet been reported, except for the silica treated with aminosilanes and dispersed into solvents for the sake of liquid-state NMR,[60] relaxation time measurements on each carbon resonance enables us to estimate the cite-specific mobility of the molecules. The high-resolution solid-state NMR is not limited to ^{13}C. A great potential of this technique is also expected using ^{29}Si and preliminary results are reported.[61-64]

Figure 21 shows a high-resolution solid-state ^{29}Si spectrum of a silica gel.[63] Three resonance lines are well resolved at -90.6, -99.8, and -109.3 ppm which can be assigned to the surface $(SiO)_2\overset{*}{S}i(OH)_2$, $(SiO)_3\overset{*}{S}iOH$ and $(SiO)_4\overset{*}{S}i$, respectively. The silicons with asterisks are responsible for the resonances. It should be noted that the silicon near a proton appears strongly, thus, the surface of the silica gel contributes a major part of the spectrum.

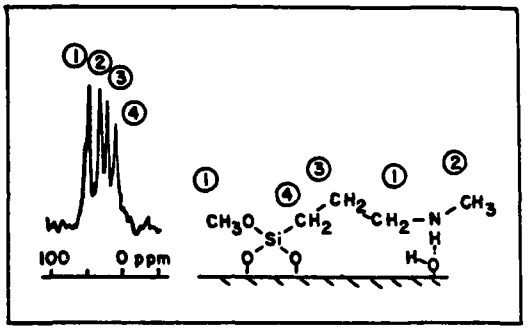

Figure 20. High-resolution solid-state ^{13}C NMR spectrum of N-methyl-γ-aminopropyltrimethoxysilane on silica gel.

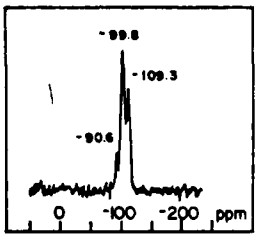

Figure 21. High-resolution solid-state ^{29}Si NMR spectrum of silica gel obtained at 11.88 MHz.

Figure 22 illustrates the high-resolution solid-state ^{29}Si NMR spectra of aminosilanes on a high-surface-area silica.[64] The 19 ppm line in spectrum A. is due to the ^{29}Si resonance of the silica gel treated with γ-aminopropyldimethylethoxysilane and the -58 and -84 ppm resonance lines are due to the silica treated with γ-APS. A large chemical shift allows us to easily distinguish the monofunctional silane with respect to inorganic functionality and trifunctional silane like γ-APS on the silica surface. Furthermore, it can be seen that the γ-APS on the surface contains a fully cross-linked $RSi(OSi)_3$ group possibly seen as -84 ppm line and a partially cured group $RSi(OSi)_2OH$ at -58 ppm. Note that the reduction of the surface monosilanol at -101 ppm and vicinal silanol at -91 ppm is due to the silane treatment.

The examples shown above clearly demonstrate the great potential of high-resolution solid-state NMR in the studies of glass surfaces and their surface treatments.

Aside from the importance of the silane interphase, the glass/silane and silane/matrix interfaces are equally important

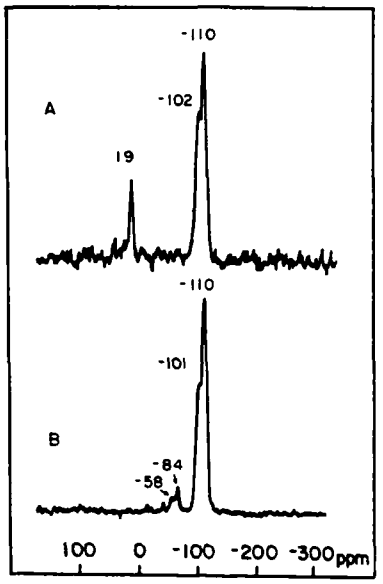

Figure 22. High-resolution solid-state ^{29}Si NMR spectra of silica gel treated with (A.) γ-aminopropyldimethylethoxysilane and (B.) γ-APS.

in considering the reinforcement mechanism. However, it is much more difficult to study these interfaces because of the negligible amount of materials involved. Nevertheless, some progress has been made. The glass/silane interface is a more well defined interface than the metal/silane or silane/matrix interface. In the case of a metal substrate, the surface oxides may dissolve into the silane layers as reported by Boerio et al. on aluminum[65] or form a complex.[65 66] The silane/matrix interface is suspected to be a diffuse boundary layer due to the dissolution of the physisorbed silanes into the matrix phase and the penetration of the matrix resin into the chemisorbed silane layers.

The metal/silane interaction has been observed as stated previously.[19] Ishida et al.[45] studied E-glass fiber/γ-MPS interface and showed that the carbonyl group of γ-MPS strongly interacts with the surface acid centers. The free carbonyl and weakly hydrogen bonded carbonyl show infrared bands at 1720 and 1700 cm^{-1} respectively. The carbonyl which is interacting with the surface acid centers gives rise to the band around 1670 cm^{-1}. Similar frequency shifts for the molecules other than silanes containing carbonyl groups were also reported.[67-69]

Ishida et al.[45] observed the surface induced polymerization of the C=C bond of γ-MPS when it is adsorbed onto E-glass fibers and dried at room temperature. After 500 hours of drying, approximately half of the C=C bonds were polymerized. It is not known, however, what effect the polymerized γ-MPS has on the mechanical performance of composites.

Using the 1670 cm^{-1} carbonyl band as a molecular probe for the interfacial silane molecules, Ishida et al.[45] determined the concentration of the γ-MPS that yields a monolayer coverage to be 0.016% by weight. However, this concentration may vary depending on the treatment conditions. Knowing the number of adsorbed molecules and the specific surface area of the fiber, they determined the area of the surface occupied by a single γ-MPS molecule to be 48$Å^2$ which is in good agreement with the expected size of molecules.

Chemical bond formation between iron and a silane coupling agent was reported by Gettings and Kinloch[70] using SIMS. The observed SIMS peak at amu=100 possibly correspondong to the $FeSiO^+$ ion. It is interesting to notice that the amu=100 peak appeared only when γ-GPS at 1% by volume aqueous solution was used as a primer. Two other silanes, namely a styrylbenzyl amine chloride functional silane and γ-APS, did not show this peak leading the author to conclude that only γ-GPS has chemical bonds at the interface. A further careful examination may be needed since the γ-GPS was coadsorbed with an equal amount of an amine catalyst while others were not. The fragment of the catalyst may give rise to the peak.

When γ-APS was used as a primer, the oxide layer was much thinner than γ-GPS primer, due probably to the decomposition of the iron oxide by the amine. This phenomenon was also reported on the γ-APS/aluminum system.[65] Even though the current densities of the Argon ion beam was kept small at around 10^{-10} Acm^{-2} so that only the first few layers are studied, the SIMS spectrum showed the elemental Fe^+ ion on the all primed surfaces indicating that the iron surface is not covered uniformly. A similar observation was made on γ-APS/Al_2O_3 system[35] as well as on γ-GPS/SiO_2 system.[71] The so-called "punch through" phenomenon as stated above is the term used to indicate electron escape of more than the usual escape depth due to the nondense portion of the film. Cain and Sacher[71] showed that γ-APS/SiO_2 system did not show the "punch through" phenomenon contrary to the work by Gettings et al.[70] The depth profile analysis of γ-APS by Auger electron spectroscopy is shown in Figure 23. As we have seen already that the structure of γ-APS is extremely sensitive and the difference may well be attributed to the conditions of the sample preparation.

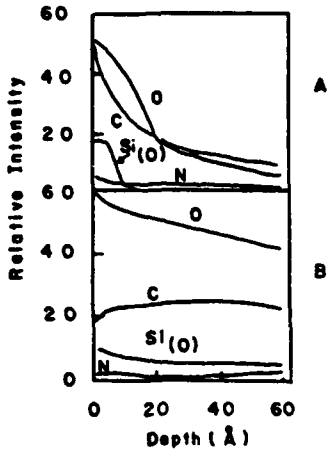

Figure 23. Auger depth profile of a silicon wafer treated with γ-APS hydrolyzed with (A) 50:50 mixture of methanol and water and (B) water. The "punch through" phenomenon is seen only in A.

Bascom[15] used an electron microscope to observe a silane film on a metal substrate. The electron photomicrograph showed a smooth appearance when the silane film was very thin. It is likely that the nonuniformity observed by ESCA, SIMS, and Auger is too small for the electron microscope to resolve.

5. The Surface of Substrates and Its Effect on the Function of Coupling Agents

In relation to the hydrothermal stability, two theories are of particular interest. Both the electrokinetic theory proposed by Plueddemann[72] and acid-base theory by Fowkes[73] emphasize the importance of the surface acidity to the structure of coupling agents or polymer matrices. The acid-base theory is essentially the same as the electrokinetic effect.

Plueddemann[72] showed that the wet strength of metal plates coated with polymers with various acidities do not show any systematic tendency. Hence, the acid-base interaction concept may be invalid when wet strength is of our interest. Since the acid-case interaction is a secondary interfacial interaction, polar molecules such as water can compete for the metal surface with the matrix resin resulting in weakening of the acid-base interaction. Accordingly, the acid-base theory may only be applicable for dry systems where little perturbation by a polar media esists. For wet systems, however, other factors have to be considered. At present, the chemical and morphological influence of the interfacial acid-base interaction with a much thicker matrix interphase

is not well understood. This effect may be an important factor when the rheological properties of the liquid polymer with a filler are considered.

The electrokinetic effect is also an interfacial effect. The surface potential at various pH is different, which influences the orientation of a silane when adsorbed. The structure of the first layer would influence the subsequent layers, and thus interfacial effects extend to a considerable distance. The mechanical consequence of the electrokinetic effect on the adhesive strength has been studied by Boerio et al.[37] Figure 24 illustrates the lap-joint strength retention as a function of the immersion time in hot water. The metal plates were treated with a dilute aqueous solution of γ-APS at various pH. The lap-joint prepared in acidic pH retained more strength than in alkaline pH. It was explained that due to the orientation of the silane caused by the electrokinetic effect, the effectiveness of the coupling agent varied. The reflection-absorption infrared spectra of γ-APS on the metal surface at various pH showed major spectral difference. This occurred most notably near the pK_a of γ-APS.

The electrokinetic effect on the adsorption characteristics of the silane is not known. Preliminary data[75] show that the amount of silane adsorbed varies significantly with pH, even though the concentration of the silane in the treating solution is the same. It has been shown that the thickness of the silane interphase influences the mechanical properties of composites.[76-78] Thus, the orientation effect may not be solely responsible for the results observed by Boerio et al.[37]

In the case of glass fibers, multiple components could exhibit various isoelectric points of corresponding oxides. It is possible, for a first approximation, to calculate the average isoelectric point of the surface of glass fibers by adding the

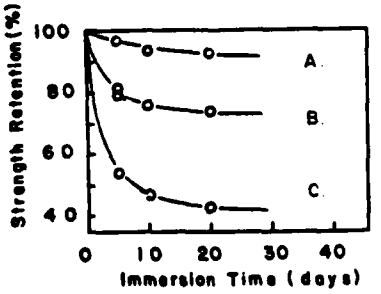

Figure 24. Strength retention of aluminum/epoxy lap-joints treated with γ-APS aqueous solution at (A.) pH = 8.5 and (B.) ph = 10.4. No silane treatment was given for (C.) Immersion test was carried out in water at 60°C.

weighted isoelectric points when the surface composition is known.[72] Problems arise if microheterogeneity exists on the surface because the coupling agent may behave differently in each domain. The averaged isoelectric point with respect to the local behavior of the silane may be different. Most solids are said to be chemically heterogeneous.[79-80] Hence, a single surface energy may not be valid to express the surface property of a solid. Penn and Bowler[81] proposed a new qualitative method to evaluate adhesion characteristics of two solids using the bar graph method where several arbitrary standard liquids were chosen and the hysteresis of the advancing and receding angles were plotted against the surface tension of the standard liquids. In Figure 25, the bar graphs of epoxy, oxidized polypropylene, and unoxidized polypropylene are shown at various surface tensions of the standard liquids. The maximum and minimum point of the bar represent the cosine of the receding angle θ_r and the advancing angle θ_a, respectively. The similarity in the bar graph (Figure 25, A and B) implies that both materials are thermodynamically similar and, thus, adhere better. The dissimilarity in the values of $\cos\theta_a - \cos\theta_r$ for each reference liquid (Figure 25, A and C) indicates poor adhesion. The single rod pull-out test shows that in fact the bond strength of the epoxy resin/oxidized polypropylene system has better adhesion with the bond strength of 304 ± 103.3 lb/in^2 whereas the epoxy/unoxidized polypropylene yields 149 ± 26.3 lb/in^2.

A further problem of an averaged isoelectric point is that mixed oxides have different surface characteristics than the individual oxides.[82] Figure 26 shows the UV-visible absorption spectra of oxides on which tetracyanoquinodimethane (TCNQ), a strong electron acceptor, is adsorbed. The oxide with an intermediate composition showed additional features which do not exist in either of the pure oxide/TCNQ spectra. Thus, simple additivity does not hold.

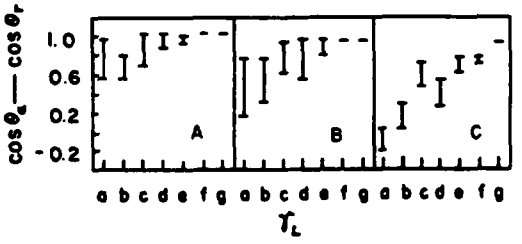

Figure 25. Bar graphs representing the hysteresis of the advancing and receding angles of various arbitrarily chosen liquids with varying surface tensions: (a) 72.8; (b) 58.2; (c) 50.8; (d) 48.2; (e) 43.9; (f) 35.4; and (g) 27.6 dyn/cm. Graphs A, B, and C represent cured epoxy resin, oxidized polypropylene, and polypropylene.

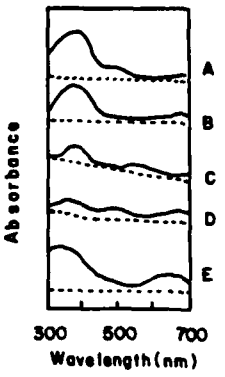

Figure 26. UV-visible absorption spectra of TCNQ adsorbed on aluminosilicate with varying silica content. Approximate silica content is (A) 100%; (B) 75%; (C) 50%; (D) 25%; and (E) 0%. Dotted lines are the aluminosilicates prior to adsorption.

6. The Coupling Agent/Matrix Interface

Copolymerization at another important interface, i.e., silane/matrix interface, was investigated by Ishida and Koenig[83] and Chiang and Koenig[84,85] on γ-MPS/polyester and γ-APS/epoxy systems, respectively. A high surface-area silica was treated with VS and γ-MPS and mixed with styrene. After polymerization of the styrene, both coupling agents had lost their C = C groups indicating copolymerization. When E-glass fiber was used as a substrate for these silanes, only γ-MPS showed evidence of copolymerization. The likely explanation is that VS does copolymerize at the interface but because of its tight packing the matrix cannot penetrate and copolymerize in the interphase. On the contrary, γ-MPS has a rather coarse interphase through which the matrix can penetrate. Also, the reactivity of the methacryl group towards styrene is higher than that of the vinyl. As a result, the major part of γ-MPS interphase copolymerized with the matrix. This is consistent with the fact that glass fibers treated with γ-MPS yield superior composites than fibers treated with VS.

When the glass surface is treated with a silane whose organofunctionality has a high reactivity toward the matrix, the curing of the matrix near the interface may locally improve or the effect of the substrate may be shielded. If the surface is not treated with a silane, curing of the matrix may be inhibited. A milled, untreated E-glass powder was mixed with a polyester at various concentrations and the polyester was polymerized at room temperature. A noticeable amount, which was linearly proportional to the glass content (Figure 27) of unpolymerized C = C bond of the

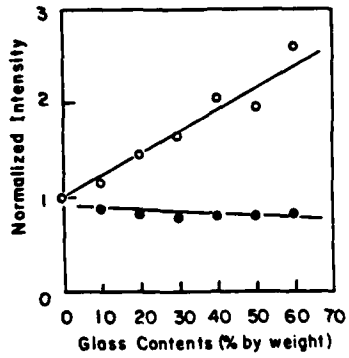

Figure 27. Amount of residual C = C groups of (o) polyester and (●) styrene at various glass content. Room temperature curing system was used and no post cure was given.

styrene was constant throughout the glass content. As Hosaka and Meguro[82] reported, and Plueddemann later advanced,[86] inorganic filler surfaces have a relative ability to terminate free radicals as listed in Table II. Since the mobility of the polyester chain is low, the influence appears strongly on the polyester only, while styrene can escape from the interfacial region and polymerize outside. Heat treatment of the composite reduces the amount of residual double bonds due to either the initiation by the reactivation of surface inorganic radicals[86] or increased mobility of the peroxide initiator.

Table II. Relative Ability of Various Fillers to Terminate Free Radicals.

Mineral Filler	Relative electron donor ability	Exotherm lowering by filler in polyester (°C)
MgO	100	24
$Al_2O_3 \cdot 3H_2O$	76	19
ZnO	47	13
Al_2O_3	38	9
TiO_2	1.6	12
SiO_2	0.11	6

The reaction between γ-APS treated surface and glycidylether of bis-phenol-A with nadic methyl anhydride as a cross-linking agent has been found to be complex.[84] Formation of amine, imide, and ethers occurs. The primary amine of γ-APS reacts with the anhydride as follows:

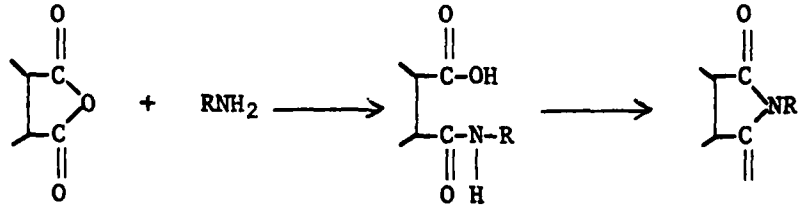

In the presence of epoxy groups, the following reaction is also possible.

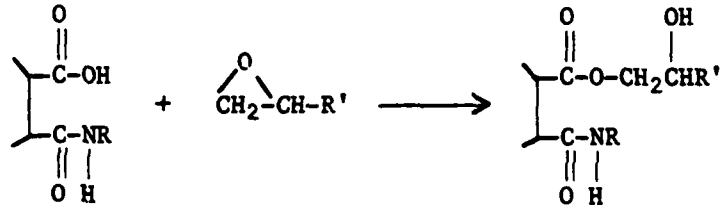

Formation of the esters, amide and imide groups were observed at the interface which were characterized by the infrared bands at 1738, 1650, and 1700 cm^{-1}, respectively, and the FT-IR difference spectrum is shown in Figure 28.

If the long chain formation or extensive cross-linking are favored for reinforcement, the imide formation is undesirable since it terminates the chain propagation. Imide formation was found to be predominant when a high-surface-area silica treated with γ-APS was reacted with 1:1 mixture of anhydride and epoxy resin.

In an attempt to eliminate the imide linkage that terminated the chain propogation, the primary amine and secondary amine functional coupling agents were compared.[85] For the primary amine γ-APS was used and N-methyl-γ-aminopropyltrimethoxysilane (MAPS) was used for the secondary amine. MAPS showed a higher reactivity than γ-APS in the absence of a tertiary amine catalyst in the epoxy resin (Figure 29). It is possible that the tertiary amine formed acts as a catalyst and accelerates the curing. Instead, the structure of the silane hydrolyzate may be different and the steric factor may cause this reactivity difference. In fact, when n-propylamine, aliphatic analogue of γ-APS, and the

hydrolyzate of γ-APS are compared for their reactivity toward epoxy resin, n-propylamine showed a much higher reactivity.

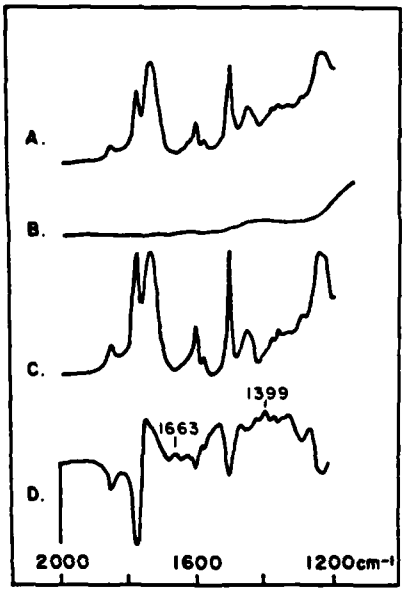

Figure 28. FT-IR spectra of glass fiber/epoxy system.

(A.) Composite (B.) E-glass fiber
(C.) Cured epoxy (D.) The difference spectrum (D=A-B-C)

E-glass fibers are treated with γ-APS. Amide band at 1663 cm^{-1} and imide band at 1399 cm^{-1} are observed.

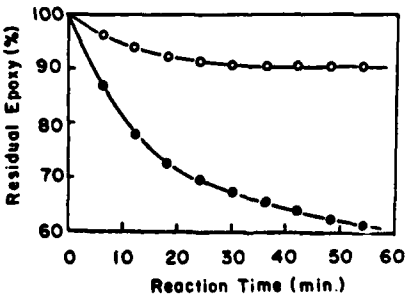

Figure 29. Residual epoxy content in glycidyl ether of bisphenol-A reacted with unhydrolyzed (o) γ-APS and (●) N-methyl-γ-aminopropyltriethoxysilane at 150°C.

Based on the findings, the authors recommend the conditions for maximizing the number of interfacial bonds. Higher curing temperatures and lower amounts of accelerators are said to increase the number of interfacial bonds, although this may not be acceptable from the practical point of view since considerations have to be made with respect to the processing of the composite.

7. The Influence of the Matrix Interphase on the Mechanical Properties

Structural gradients within the matrix near the interface have been studied by Jonath and Crowley[87] using an ultrasound technique. A 20 MHz ultrasonic transducer was used to measure Rayleigh wave[88] at the adhexive surface and they calculated the shear modulus of the adhesive layers at various thicknesses using measured density profile and shear speed. An example is shown in Figure 30 where epoxy adhesive is used for aluminum joint. Near the metal surface within 200 μm, the shear modulus decreases appreciably. In order to calculate the shear modulus, the density of the adhesive at the particular thickness should be known. Within the experimental errors, there was no density variation as a function of distance from the metal surface. It has been reported, however, that rarefied matrix interphase exists near the surface of the glass fibers.[89-92] It is important to mention that, even though the density was assumed constant, the rarefied layer would have a lower speed of sound and thus result in a more dramatic decrease in the calculated modulus near the metal surface. The calculated modulus G is expressed as $G = \rho C_s^2$ where ρ is the density and C_s is the shear wave speed.

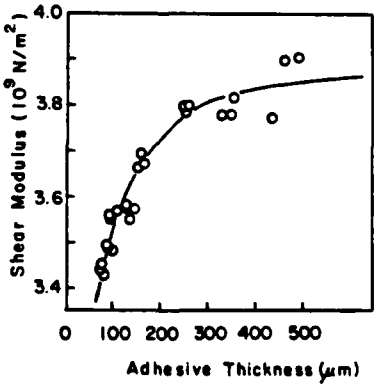

Figure 30. Shear modulus calculated from the shear speed and density measurements on the various thicknesses of epoxy adhesive polished metallurgraphically. The frequency of ultrasound used was 20 MHz. The zero thickness represents the metal surface.

The majority of reported values for the thickness of the matrix interphase falls within the 10^{-3} - 1 μm range[1] but the ultrasound results indicate considerable thickness. It is possible, however, that because mechanical properties are sensitive to minor structural variations and the ultrasound technique probes properties related to the elastic properties of the material, the reported value represents the true profile of mechanical properties of adhesives near the interface. On the other hand, most of the techniques used in the past to measure gradients were aimed at the detection of structural differences that influence the mechanical properties considerably. The ultrasound results[87] were consistent with the thermally stimulated current (TSC) measurement (Figures 31 and 32) where the structural gradient extends to approximately 200 μm from the substrate surface.

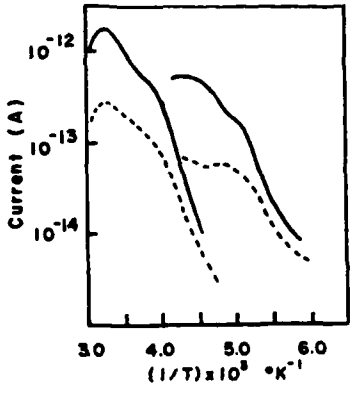

Figure 31. Thermally stimulated current (TSC) spectra of the same epoxy adhesive as in Figure 30. The solid line is the bulk epoxy and the dotted line is the epoxy in the matrix interphase.

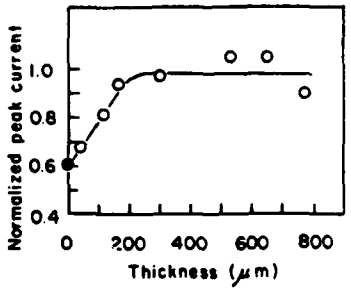

Figure 32. The TSC intensity of the peak at 5×10^{-3} °K^{-1} in Figure 31 for epoxy adhesive with various thicknesses by metallurgraphic polish. The data point shown as a closed circle was obtained for a fractured specimen and was measured on the epoxy remaining on the metal surface.

The observation of less rigid matrix near the substrate may have a significant consequence in light of Tryson and Kardos' work,[93] and Drzal et al.'s results.[94] Tryson and Kardos applied a soft epoxy matrix of approximately 0.5 μm thick around a monofilament and the mechanical properties showed a remarkable improvement as compared to the fibers without soft innerlayers. The results are summerized in Table III.

Table III. Effects of a Ductile Innerlayer on the Various Mechanical Properties of Fiberglass Reinforced Epoxy.

Mechanical property	Improvement
Transverse tensile strength	67%
Transverse strength after water exposure (2-hour boil)	57%
Torsional fatigue life	1000%
Interlaminar shear strength	40%

These improvements can be attributed to two fundamental functions of the inner layer. First, the inner layer prevented reduction of the fiber strength during handling. Without the inner layer, 24% of the initial strength was lost while with the inner layer, no detectable damage was observed. Secondly, the inner layer acts as a "bumper" so that it reduces the stress concentration factor in the matrix and prevents direct fiber contact resulting in a reduction of local matrix strain. These results are in accord with the theoretical prediction by stress analyses.[95]

It is interesting to point out that the ductile inner layer is not the only one that has been shown to be effective. Graphite fiber involves many factors that are beyond the scope of this article and readers should refer to the recent book by Delmonte[96] and papers by Drzal et al.[97-99] for the extensive treatment of these subjects. However, Drzal et al.'s work[99] on meta-phenylene diamine-cured diglycidyl ether of bisphenol-A which is reinforced with a graphite fiber seems relevant to the role of the matrix interphase in the reinforcement mechanism. The oxidized graphite fiber was coated with the epoxy without the cross-linking agent. Then the epoxy with the curing agent was applied and subsequently cured. The coated fiber showed an improvement in interfacial

shear strength by about 13% over the oxidized fiber. They explained that the coating is deficient of the curing agent and, during the cure of the surrounding epoxy, the curing agent migrated into the coating and cured it at much less concentration. The resultant coating is more brittle than the surrounding matrix bulk and the brittleness was said to be more efficient for stress transfer to the fiber.[100] The fracture would initiate in this brittle coating rather than the glass/matrix interface, which is the situation analogous to the ones reported by DiBenedetto and Scola[101] and Sung et al.[78] for glass/silane/thermoplastic systems.

Both soft and brittle matrix interphases are reported to improve the mechanical properties of composites by altering the fracture modes. Hence, one method is more effective than the other on a specific mechanical property. For example, the improvement in torsional fatigue using a soft interphase is dramatic and, in general, the soft interphase would result in better performance for fatigue properties than the brittle interphase.

The significance of these reports is not only to demonstrate the importance of the matrix interphase to the properties of composites, but also to understand the mechanical consequence of the silane interphase, the chemisorbed and physisorbed silanes to the matrix interphase. If the silane interphase is to modify the matrix interphase, there must be an optimum combination of silane and matrix to form the matrix interphase with proper mechanical properties since the relative rigidity to the matrix bulk determines the effectiveness of the interphase.

It is, therefore, essential to evaluate the mechanical properties of the interphase. Unfortunately, due to the technical difficulties, few studies have been reported.

The effect of ductile or rigid inner layer is analogous to the use of silane primer and finish. Usually primer is the term used for a relatively thick coating on the order of submicrometer to micrometers while the finish is used for the thickness range of nanometers. Thus, the reinforcement mechanisms have to be considered separately. Historically, the deformable layer theory[102] was proposed as one of the reinforcement mechanisms. Because of the opposition stating that the thickness of the silane layer is not sufficient to be counted as an effective mechanism, the theory lost its support. However, this theory is essentially the same as the inner layer concept described by Tryson and Kardos[93] and the silane primer may function as the ductile inner layer. In fact, the prehydrolysis of a concentrated silane alcohol solution[13] may support this explanation. Upon prehydrolysis with a small amount of water, the silane forms an extensive open structure suggested

by the gelation phenomenon. After leaving the prehydrolyzed silane for more than several hours, there may be a rearrangement in the siloxane structure or hydrogen bonded silanols so that the silane eventually forms more cyclic siloxane, thus creating a ductile primer. It is known that if the freshly hydrolyzed primer is used it is ineffective, because the siloxane structure is expected to be an extensively open structure leading to a too brittle film.

With regard to the film quality of the primer or the modified properties of the rather thick matrix interphase, a new method of improvement in composite strength is of particular interest. Mayer and Newman[103] reported that the use of chlorinated paraffin is effective for improving the mechanical properties of particulate-filled thermoplastics. Plueddemann et al.[104] evaluated the paraffin and silanes to the strength of filled polypropylene (Table IV).

Table IV. Flexural Strength of Wollastonite Filled Polypropylene with Several Combinations of Additives.

Surface treatment	Flexural strength (psi)	
	Silane only	Chlorinated paraffin and MgO added
None	7740	8070
γ-APS (0.5 wt %)	7750	8840
Styryl benzyl functional silane	7860	9220
Azide functional silane	9580	9620

•Unfilled polypropylene has flexural strength of 7500 psi.

••Above results were obtained using 35% fibrous wollastonite filled polypropylene.

Presently, the exact reinforcement mechanism is not known. Possible cause can be hypothesized. First, the chlorinated paraffin may dehydrochlorinate to form conjugated double bonds that may undergo further polymerization leading the covalent bond formation to alter the resin structure. The chlorinated paraffin,

however, does not show major dehydrochlorination at around 200°C within 15 minutes, the time which mica and wollastonite showed an improvement in injection molded composite. The dehydrochlorination may have been catalyzed in the presence of the filler and the magnesium oxide added as a scavenger for HCl. Second, the addition of paraffin may alter the morphology of the resin at the interface. Preferential adsorption of either the paraffin or silane on a substrate may take place. It is reported that mica[105] and other inorganic surfaces[106,107] show epitaxial crystallization. The ability to epitaxially crystallize may be altered by the shielding effect of the small molecules that cannot be crystallized.

Stevenson and others[108] reported the reinforcement properties of mica and wollastonite reinforced polypropylene with chlorinated paraffin treatment (Figure 33). Their results show that, depending on the filler, the molecular weight of the effective chlorinated paraffin varies; the liquid paraffin is more effective for wollastonite while a higher molecular weight paraffin is better for mica. Aside from possible chemical coupling at the interface, it is likely that several competing effects are taking place. For example, plasticization, alteration of the interfacial morphology, and mechanical interlocking are possible candidates.

For a smooth surface such as mica, interfacial wetting may not be as big a problem as for the rough surface of wollastonite. Smaller molecules may be a better solvent for polypropylene to wet the rough surface of wollastonite and yield better mechanical

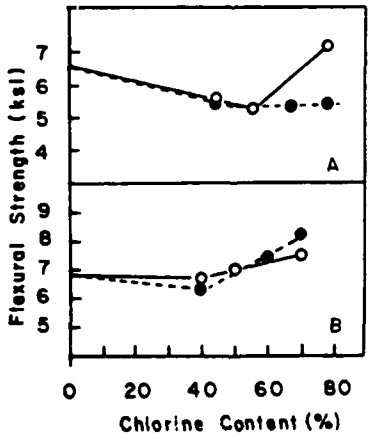

Figure 33. Effect of chlorine content on the flexural strength of (A.) 35% mica and (B.) wollastonite filled polypropylene mixed with chlorinated paraffin with chain lengths of (o) $C_{22} - C_{30}$ and (●) $C_{10} - C_{12}$.

interlocking by which plasticizing effect is suppressed. On the contrary, the smooth surface of mica does not require too much plasticizing effect, but effective shielding of the epitaxial effect of the mica, creating finer crystallites, may be the dominating effect.

One cannot exclude the chemical coupling effect from the above factors. Possible catalytic effect of added MgO for dehydrochlorination was described[108] (Figure 34) though a small amount of alkaline inorganic oxides act as stabilizers for PVC. The addition of MgO showed little change in wollastonite filled polypropylene whereby mica showed appreciable improvement. With the smooth surface of mica, chemical coupling will improve the strength over the uncoupled sample, as compared to the insensitive feature of the wollastonite system where mechanical interlocking dominates. This is consistent with the above hypothesized reinforcement mechanism. Too much scavenging may be harmful as pentaerythritol, a stronger scavenger than MgO, decreased the mechanical strength of the composite as the concentration increased. It is possible that the strong scavenger triggered the "zipper effect" to yield more conjugated paraffins and made the molecule stiffer, hence led the paraffin to be an ineffective wetting aid.

The sensitivity of the reinforcing effects to the chlorine content of paraffin may be related to this scavenging effect in addition to the solubility difference among various chlorinated paraffins. The paraffin with both high and low chlorine contents may not form long conjugation induced by dehydrochlorination. It it interesting to notice that the minimum reinforcement effect is observed around 40 - 50% chlorine content, which is statistically favorable for yielding longer conjugation.

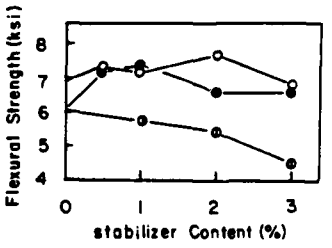

Figure 34. Effect of stabilizer content on filled polypropylene:

- o wollastonite and MgO
- ● mica and MgO
- ◖ mica and pentaerythritol

All the systems have 2% by weight chlorinated paraffin loading.

All these explanations are still hypotheses and further fundamental studies are needed to distinguish the function of the individual mechanism.

8. Silanes on Particulate Fillers

In general, particulate fillers are treated by dry blending a silane as a neat liquid or an organic solution. Because the silane is not hydrolyzed to organosilanetriol, the structure of the coupling agent interphase is quite different from the silane which is adsorbed from a dilute aqueous solution. Compared with the remarkable progress in elucidating the structure of the silane adsorbed from the aqueous solution, few fundamental studies appeared on the dry blended silane. Nonetheless, interesting new findings have been reported, which may lead us to a better understanding of the role of surface treatment.

Nakatsuka et al.[109] applied infrared spectroscopy and gel permeation chromatography (GPC) for studying the structure of γ-MPS on fillers such as $CaCO_3$, phospholic acid-treated $CaCO_3$, and clay. A mixture of water and methanol (2 ml:8 ml) was mixed with 1 ml of silane and sprayed on 105 g of filler and blended. After drying and heat treatment at 80°C for 2 hours, the amount of recoverable silane by decomposing $CaCO_3$ was measured. They found that a significant portion of the silane evaporated during the drying process.

The silane was extracted from $CaCO_3$ and clay by styrene monomer. Approximately the same amount of silane was extracted from both fillers but the infrared spectra indicated a major structural difference. The alkoxy group of γ-MPS from clay was more hydrolyzed and showed more siloxane formation than from $CaCO_3$.

GPC curves for tetrahydrofuran (THF) extracts of γ-MPS from $CaCO_3$ (Figure 35) and clay (Figure 36) show that there is a large amount of low molecular weight fraction existing on $CaCO_3$. These low molecular fractions are possibly due to the monomer through tetramers. Increasing the amount of silane added did not significantly influence the high molecular weight fraction. On the contrary, the γ-MPS from clay showed almost no low molecular weight fraction when the amount of silane added was low. Increasing the amount of silane shifted the GPC curve toward lower molecular weight but no monomeric silane was observed.

Treatment of $CaCO_3$ surface by methanolic phosphoric acid reduced the amount of low molecular weight fraction and shifted the high molecular weight fraction to an even higher position. A comparison is shown in Figure 37 where THF extracts of γ-MPS from three different surfaces are shown. Note that the silane

to filler ratio is approximately the same. They observed that the mechanical and physical properties of the particulate filled vulcanized rubber improved with the filler which showed a high molecular weight fraction.

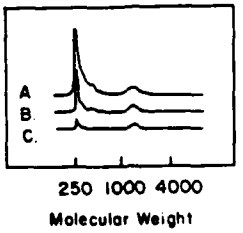

Figure 35. GPC curves of γ-MPS extracted by THF from silane-treated $CaCO_3$ with silane loadings at
(A.) 16.3%, (B.) 8.0%, and (C.) 2.5% by weight.

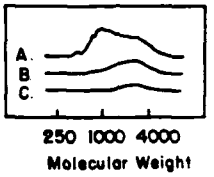

Figure 36. GPC curves of γ-MPS extracted by THF from silane-treated $CaCO_3$, which was pretreated by phosphoric acid, with silane loadings at
(A.) 15.1%, (B.) 7.8%, and (C.) 2.7% by weight.

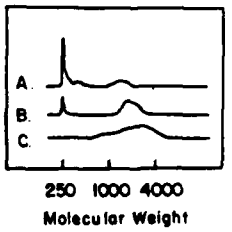

Figure 37. GPC curves of γ-MPS extracted by THF from
(A.) $CaCO_3$,
(B.) $CaCO_3$ pretreated with methanolic solution of phosphoric acid,
(C.) clay
at silane loadings of 8.0, 8.2, and 7.8% by weight respectively. The pH of aqueous suspension (0.05 g/ml) of $CaCO_3$, phosphoric acid treated $CaCO_3$, and clay were 9.30, 7.73, and 4.76, respectively.

Dry blending results in a major portion of physisorbed silane leaving approximately a monolayer quantity of chemisorbed silane whose coverage is imperfect on the filler surface. Although an appreciable amount of water is usually existent on the filler surface and it may hydrolyze the alkoxy group of silane, water is not a necessity for a chemical reaction at the interface. The following reaction is possible in the absence of water.

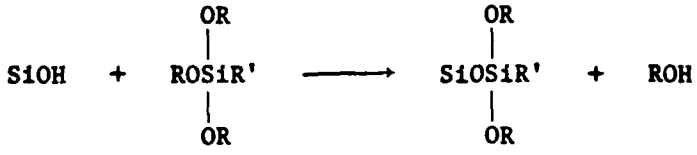

In fact, model studies by Dreyfuss et al.[110,111] using trimethylmethoxysilane and triethylsilanol showed the reaction products analogous to the above example. This type of reaction was shown to occur readily, though other types of reaction proceeded slowly and there seems to be a dynamic equilibrium among them.

Similar information on the physisorbed silane was obtained by Rosen and Goddard[112] using the filler desorption test (FDT) which involves the surface tension measurement of the air/water interface after addition of a silane-treated filler. Since the major portion of silane is physisorbed for a dry-treated filler and the silane is rather hydrophobic, the surface tension of the water changes immediately after the addition of the silane-treated filler in the water bath. Although the initial intention of the work was to evaluate water attack on the silane, and some qualitative correlation with the wet performance of composites are seen, this technique does not measure the chemical attack on the silane nor the time scale and temperature used to justify the chemical reaction when compared with the concentration variation of the silanol as a function of time.[50] Rather, it examines the physical consequences of the various silane structures.

FDT yields qualitative information on the molecular weight and its distribution of the physisorbed silane, which is reflected on the solubility of the silane oligomers. The more hydrophobic the oligomer is, the more pronounced the influence on the surface tension. The larger oligomer requires longer time to desorb, thus the FDT curve changes slowly while a small oligomer desorbs immediately. The advantage of this technique is its sensitivity. Because it requires a negligible amount of material to cover the water surface at a monolayer level, only a small amount of silane desorption is required to detect the structural difference.

FDT curves of γ-MPS on particulate silica, aluminum trihydrate and $CaCO_3$ are shown in Figure 38. As it can be seen from the

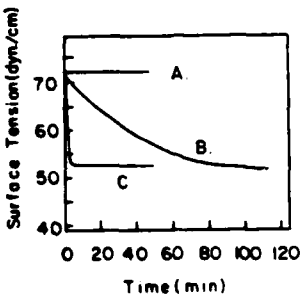

Figure 38. FDT curves of (A.) silica, (B.) aluminum trihydrate, and (C.) $CaCO_3$, treated with γ-MPS by dry blending 1% by weight of filler as a solution of 9:1 mixture of methanol:water. The fillers were heat treated at 100°C for 1 hour.

figure, the quick change in the surface tension of $CaCO_3$ and the possible saturation of the water surface with the floating silane indicate the desorption of small oligomers, which is consistent with the previously stated GPC results.[109] Silica, on the other hand, showed almost no desorbed silane. The surface acidity of silica and clay is similar. Also, the GPC curve showed no small molecular weight fraction.[109] The higher molecular weight fraction observed in the GPC spectrum may not desorb during the FDT experiment, though the silane is physisorbed.

Evidence of imperfect coverage has been obtained by ζ-potential measurement of silane-treated alumina as shown in Figure 39.[113] The dry-treated alumina showed a ζ-potential curve which was similar to untreated alumina. The isoelectric point of the untreated, dry-treated, and wet-treated alumina were 8.7, 7.9, and 3.4, respectively. Perfect coverage would result in a rather negative surface similar to the silica surface as is the case for the wet-treated alumina. It is known that silane molecules on the surface have residual silanol groups even after drying at elevated temperatures.[41,42] Thus, the silane-treated, perfectly covered surface resembles that of silica. Similarity of dry-treated alumina with untreated alumina indicates that in spite of the amount of silane added, which is sufficient to yield more than a monolayer coverage, the alumina surface is partially exposed and the silanes are aggregates rather than uniformly distributed film. This observation is consistent with the FDT curves for the dry- and wet-treated alumina where the dry-treated alumina showed quick change in surface tension.

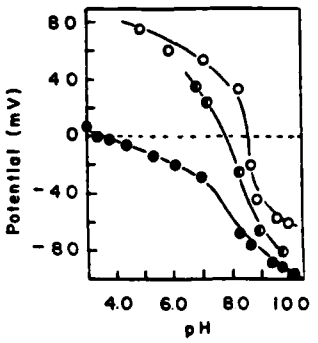

Figure 39. ζ-potential of alumina treated with γ-MPS with various treatment methods:
o no silane ◐ dry-blending ● slurry treatment

9. New Coupling Agents

In addition to widely used silane coupling agents, new coupling agents have appeared. A series of titanates have been reported by Monte and Sugerman[114-119] to be good adhesion promoters and processing aids. Although improved wet strength retention of $CaCO_3$ filled polypropylene was reported,[117] titanates are believed to be processing aids that control the viscosity of a filled polymer rather than a true coupling agent that improves the wet strength of the composite. However, dry strength may be improved. A comparison was made between a titanate and a silane for their wet strength and its retention.[72] The silane showed better performance under wet conditions than the titanate, possibly due to the hydrolysis of the TiOC bond that connects the titanium atom and the organofunctionality. Limited data on titanates necessitate further studies before any conclusions are made.

No detailed studies on the molecular structure of titanates have yet been reported. A preliminary report by Sung et al.[78] states that they observe no structural change when a titanate is deposited on a Al_2O_3 plate. When the sample was heat treated at 140°C the infrared spectrum showed some changes due possibly to decomposition of the titanate. Since the alkoxy group of the titanate used was an isopropoxy group, which is relatively stable in air compared to widely used silane coupling agents which have alkoxy groups of a primary alcohol, brief exposure to air does not lead to major hydrolysis and subsequent condensation. A report by Han et al.[120,121] shows the role of coupling agents in composite processing. It is obvious that the processability improves in the presence of a coupling agent. However, Han et al.'s results indicate that the effect on the processability depends on the type of

coupling agent used. As they pointed out, it is difficult to predict the rheological effects of a specific coupling agent due to the lack of information on the molecular structure of the coupling agent at the interface. The molecular structure/ rheological property correlation of the filled polymer has not been studied to date.

Kim and Fan[122-124] further studied the rheological aspects of $CaCO_3$ filled polypropylene with a titauate. They found that the activation energy ΔE of the viscous flow is independent of the titanate concentration and the filler content at a fixed shear rate or shear stress. Over the range of shear stress studied, ΔE was nearly constant whereby ΔE decreased with increased shear rate. The reported ΔE's with respect to the filler content, shear rate, and shear stress are listed in Tables V and VI.

Table V. Activation Energy of Calcium Carbonate Filled Polypropylene Melt with a Titanate at Various Shear Rates.

Log shear rate	$CaCO_3$ content (wt %)			
	0	20	40	60
0.5	7.09	7.06	6.93	7.12
1.0	5.87	6.17	6.09	6.43
1.5	5.17	5.40	5.35	5.65
2.0	4.38	4.17	4.56	4.98
2.5	3.97	3.52	4.07	4.02

Table VI. Activation Energy of Calcium Carbonate Filled Polypropylene Melt with a Titanate at Various Shear Stress.

Log shear stress	$CaCO_3$ content (wt %)			
	0	20	40	60
4.9	10.22	10.26	10.92	10.08
5.2	10.21	10.26	10.21	10.04
5.5	10.18	10.17	10.17	10.43
5.8	9.87	9.65	10.53	10.60

New silane coupling agents were also synthesized in recent years. Ishida et al.[125] reported a silicon phthalocyanine compound as a potential coupling agent that posses high hydrothermal stability. The silane is designed to function as a monolayer and the bulky phthlocyanine ring and relatively inert siloxane bond due to pentacoordinated silicon atom are believed to promote hydrothermal stability. Various functional groups on the central silicon as well as ring substitution are being studied.

Silanes for high temperature applications are also reported by Arkles and Peterson.[126] Introduction of a benzene ring between the silicon atom and the functional group promote thermal stability of the organic portion of the molecule.

Eib et al.[127] utilized plasma polymerization to modify surfaces. Plasma polymerized silane on a substrate results in a quite different structure than either the dry or wet treatment described earlier. High controlability in thickness and morphology are some of the advantages of this technique.

Kokubo et al.[128] synthesized various silanes and studied the mechanical properties of the composite. Among many silanes synthesized, qumenetrimethoxysilane is of particular interest since this does not possess a usual organic reactive group. Nevertheless, the composite made with an epoxy showed good dry and, surprisingly, wet strength.

NEW CONCEPTS

A. Interpenetrating Networks

The chemical bonding theory successfully explains many phenomena observed for composites. However, some evidence suggests that the chemical bonding theory alone is not sufficient and needs to be modified. For example, a monolayer of silane usually does not yield an optimum mechanical strength. Contamination of the surface, entrapped air bubbles, and imcomplete coverage of the surface were often considered to be responsible for this. However, reproducibility of the optimum concentration of the silane treating solution and the thickness resulting from the optimum concentration imply that none of these factors is likely to be the major factor. Furthermore, a well known example of inferiority of a vinyl functional silane to γ-MPS, in spite of the fact that both VC and γ-MPS are capable of copolymerization at the silane/matrix interface,[42] indicates that copolymerization with the interphase is important. Further circumstantial evidence is described elsewhere.[104]

Plueddemann et al.[104] suggested that interpenetration may be an important factor in the reinforcement mechanisms. Ishida and Koenig[50] also suggested intermixing of the coupling agent and the matrix. There are some experimental results on the molecular level that indicate the occurrence of interpenetration.

Ishida et al.[83] studied the chemical reaction of γ-MPS with styrene matrix. The FT-IR difference spectrum showed the frequency of the carbonyl group of γ-MPS shifted upon polymerization of the matrix. The frequency of the polymerized γ-MPS was different from the homopolymerized γ-MPS without the matrix indicating copolymerization took place. Copolymerization did not occur in the VS interphase. A schematic diagram for these observations is shown in Figure 40.

An indication of interpenetration was also observed on γ-APS/epoxy system by Chiang and Koenig.[84] Judging from the infrared intensity of the imide, amide and ester formed after the polymerization had taken place, the reactions were not limited to the interface.

There are two kinds of intermixing which involve penetration of the matrix resin into the chemisorbed silane layers and the migration of the physisorbed silane molecules into the matrix phase. The function of these two different structures in the reinforcement mechanisms is not known at the present time. Evidence of both structures was observed. Glass fiber treated with γ-MPS was polymerized in styrene monomer. Styrene washed away the physisorbed silane and polymerized within the chemisorbed silane layers.[50]

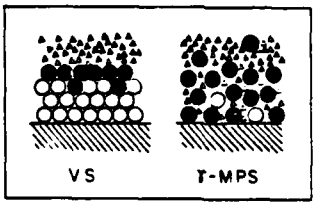

Figure 40. Schematic diagram of the silane interphase which consists of VS and γ-MPS showing interpenetration and copolymerization in the γ-MPS layers.

o unpolymerized silane

● polymerized silane

Δ styrene

Existence of physisorbed layers are well documented. Schrader et al.[43] observed that γ-APS on a glass surface can be extracted with cold water readily. Johannson et al.[44] reported the reduction of γ-MPS on E-glass fiber after a toluene wash, which was also confirmed by FT-IR study using THF wash.[45] Ishida et al.[45] studied quantitatively the amount of physisorbed γ-MPS and showed that the content of physisorbed silane is sensitive to the structure of silane in solution. Boerio et al.[65] also observed silane that can be washed away by an organic solvent. Sung et al.[78] showed migration of silane into polyethylene phase by the ESCA analysis. They observed that failure occurred in the polyethylene phase when the silane was fully dried. An optimum peel strength was observed at relatively high concentration of the silane (Figure 41). Hence, it is well established that a significant amount of physisorbed silane exists even on glass fibers treated with dilute aqueous solutions. As stated earlier, dry blending increases the content of the physisorbed silane dramatically.

The importance of the physisorbed silane to the reinforcement mechanism has not been recognized, nor the effect on the processability studied. There seem to be conflicting indications as to the function of the physisorbed silane layers on the mechanical properties. DiBenedetto and Scola,[101] using SIMS, investigated the fracture specimen of the S-glass/γ-APS/polysulfone system. The model study using a glass slide showed that the fracture always occurred 30Å inside the polysulfone matrix. One can interpret this as an indication of the strengthened layer due to the migration of the physisorbed silane into the matrix as observed in the case of polyethylene,[78] or the morphology has been changed due to the silane layers.

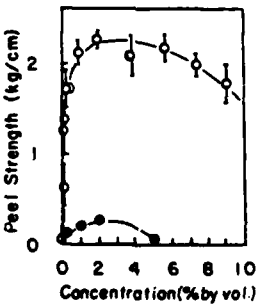

Figure 41. Peel strength of polyethylene on $A\ell_2O_3$ plate which was treated with γ-APS and a titanate at various concentrations.

A silane-treated mica eluted with methanol always yielded a stronger composite than as-treated fillers.[128] According to this study, it seems desirable to eliminate the physisorbed silane for a better mechanical performance. If the intermixing of the physisorbed silane with matrix helps strengthen the composite, it is difficult to explain the weakness of injection-molded glass beads filled polyester as compared to compression-molded composite. Since the degradation of the reinforcement is minimal in this case, the difference arises mainly because of the disruption of the interfacial structure which results from the high shear in injection molding. It is possible, however, that the physisorbed silane is carried out deep into the matrix phase due to the intense mixing of the injection molding process.

The variation of mechanical performance in the silane/matrix system indicates that an additional mechanism is necessary to explain the observed phenomenon. The interpenetrating networks theory is proposed to be one of the important reinforcement mechanisms in addition to the chemical bonding theory. A synergism of these two mechanisms seems particularly important in composites with thermosetting matrices. It is not known, however, as to the extent of chemical bonding in the thermoplastic matrices. Also not known is the number of chemical bonds that is necessary to observe appreciable reinforcement. Clearly, solubility or compatibility of the silane and the polymer matrix seem more important in thermoplastic matrices;[129] but, chemical reactivity adds additional strengths as shown in Figure 42. There is some indication that even a small amount of chemical bonding is effective for good mechanical performance. Figure 43 shows the dry and wet strengths of reinforced polystyrene where copolymers of styrene and a silane were used as polymeric coupling agents. When the molecular weight of polystyrene between two silane molecules is about 1000, good reinforcing effect was observed indicating a relatively small number of bonds can be effective. Effect of surface treatment on the morphology of the matrix and fracture mode at the interface are important in understanding the validity of the above theories.

B. Onset Concentration of Association

It is clear that the structure of the silane interphase affects the mechanical performance of composites. However, the importance of the structure of silanes in solution to the mechanical properties has not received the extensive attention it deserves. It is largely due to the difficulty in studying the dilute aqueous solutions and the lack of knowledge of the structure of silane interphase. With the increased understanding of the silane

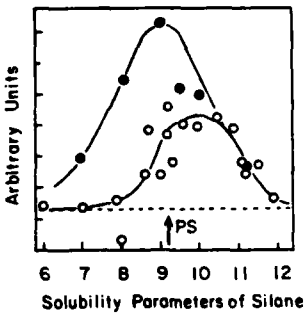

Figure 42. Glass cloth reinforced polystyrene with various silane coupling agents. Overall mechanical performance was evaluated as total rating as an internally consistent, relative measure as a function of stability parameters of the organic portion of the silane. Open and closed circles represent unreactive and potentially reactive silanes. The arrow shows the solubility parameter of polystyrene.

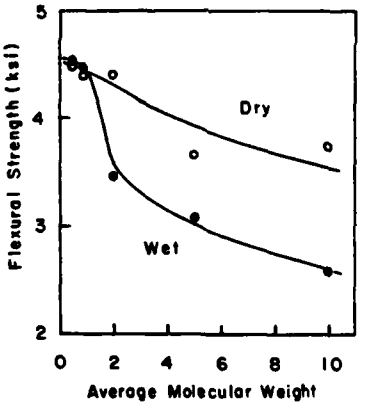

Figure 43. Flexural strength of glass cloth reinforced polystyrene with polymeric silane-treated glass: the silane to styrene ratio was varried so that the molecular weight of the polystyrene between two silane molecules becomes from 500 to 10,000 as shown as average molecular weight.

interphase, the importance of the silane structure in aqueous solutions can now be evaluated.

Hydrolysis of silanes was studied by laser Raman spectroscopy by Shih and Koenig.[3] They observed fast formation of silanetriols

and subsequent slow condensation of γ-MPS in water. Laser Raman spectroscopy has a distinct advantage in studying organosilanetriols because the symmetric stretching mode of the silanetriol falls into a very narrow frequency region with strong intensity (Table I). In general, trialkoxy groups show the symmetric $CSiO_3$ stretching mode in the range 700 - 600 cm^{-1} whereas the same mode for organosilanetriols appear in the range 730 - 630 cm^{-1}.

By observing the half width at half height of the Raman line at 684 cm^{-1} due to vinylsilanetriol, Ishida and Koenig[46] showed that the silanetriol interacts via a hydrogen bonding between silanols at above 1% by weight. As previously termed, this onset concentration of association coincided with the breakpoint of the silane up-take in E-glass fiber and moreover, with the transition at which the residual silanol content rapidly increased, when the silane-treated glass fibers were dried at room temperature. A heat treatment at elevated temperatures did not eliminate the residual silanol completely for the relatively thick silane layers. As mentioned earlier, a plasma polymerized silane showed a high degree of cross-linking and low SiOH concentrations.[130]

A schematic diagram of the structure of silane in aqueous solutions at above and below the transition concentration is shown in Figure 44 where defect formation and perturbation of the organization are seen due to the associated monomer. The oligomer should appear above this concentration. The resultant organization in the coupling agent interphase then influences the penetration of the matrix into the silane. Furthermore, the content of cyclic polysiloxane would be influenced. Cyclic polysiloxane is expected to contribute little in promoting the strength of the silane interphase. It is likely that the mechanical property of the composite with a silane above the transition concentration may not be optimum. Since many other factors may be involved in a complicated manner, there may not be a straightforward correlation. However, this transition concentration may serve as a reference concentration for the study.

The direct correlation of the solution structure and the silane up-take have been observed on other systems.[45,11] E-glass fibers with γ-MPS and γ-APS showed the breakpoints in the silane up-take around 0.4 and 0.15% by weight, respectively, as shown in Figure 45 and Figure 46. In the case of γ-APS the oligomer content increases significantly above the transition because of the self catalyzed silanol condensation. This transition will be influenced by the addition of other components such as surfactants, lubricants, catalysts, and other processing aids, thus, it should not be regarded as a universal constant.

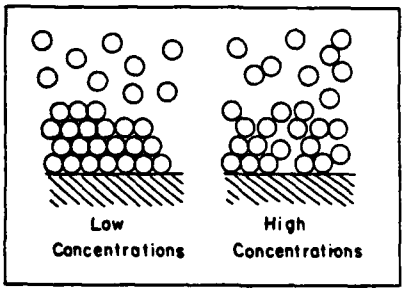

Figure 44. Schematic diagram of silane molecules in an aqueous solution at the concentrations above and below the onset of association: at above the onset concentration, associated monomers are seen and defect formation within the silane interphase is illustrated.

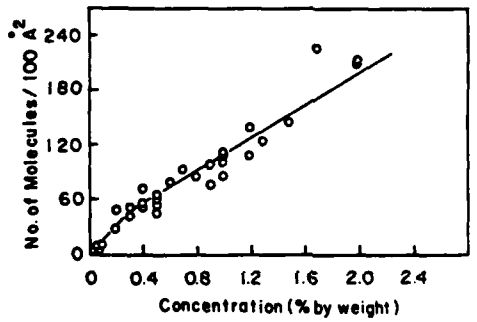

Figure 45. Up-take of γ-MPS by E-glass fibers at various concentrations of silane treating solutions.

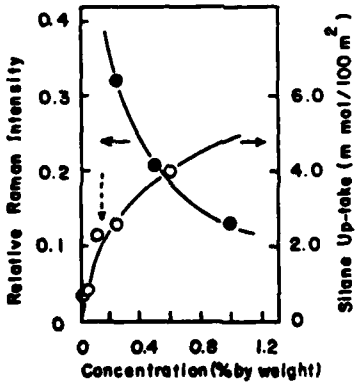

Figure 46. Up-take of γ-APS by E-glass fibers at various concentrations of silane treating solutions measured by radio-isotope technique (Reference 44) represented by open circles; the closed circles show relative Raman intensity of the silanetriol line at 712 cm^{-1}, which is compared to the ethanol line as a reference.

C. Hydrothermal Stability

It has long been believed by some researchers that silane films repel water thus promoting hydrolytic stability. As Bascom stated through his contact angle measurements,[15] silane films are porous enough so that water can penetrate with ease. Another indication is that water permeates along the interface several hundred times faster than transverse direction through the matrix. It is, therefore, likely that water is present at the interface in most cases for hydrolytic degradation when we study the humidity effect on composites. The state of water, either an isolated molecule or condensed water, may be an important variation.

There is some evidence that the hydrolysis of the siloxane network is independent of the silane structure as far as enough water is available for hydrolytic attack. Three silanes, γ-MPS, VS, and CS are compared for their desorption characteristics.[50] Although the desorption curve showed a remarkable difference because of the difference in solubility of the silane oligomers that are produced as a result of hydrolysis, the times necessary to significantly hydrolyze the siloxane networks at a given temperature were approximately the same.

It took 600 hours for γ-MPS before it reached the silane thickness where extensive organic linkages prevented the desorption as a result of the surface induced homopolymerization. For VS, the threshold period observed before the initiation of desorption ended at around 600 hours. Finally, for CS, the intensity of the SiOH band at 890 cm^{-1} in the FT-IR difference spectra reached the maximum within 600 hours and no further increase was observed due to the equilibrium between the silanol and siloxane groups. Because of the hydrophobicity of the cyclohexyl group, the silane did not desorb. Hence, although the desorption characteristics are determined by the hydrophobicity of the organofunctionality and the degree of open structure, the siloxane networks of all silanes were hydrolyzed extensively within about 600 hours in water at 80°C, which corresponds to 48 - 72 hours of boiling experiment in severeness. It is tempting to speculate that hydrothermal stability of the composite may be especially sensitive to the structure of the interpenetrating networks since, in general, these are unhydrolyzable.

A recent report by Andrews et al.[130] showed that the hydrolysis rate constant k' decreased rapidly as the concentration of silane increased to around 0.1% by weight (Figure 47). They used a disc shaped adhesive specimen[132,133] for their studies on the adhesion of epoxy on Pyrex® glass. The k' is defined as the rate of disruption of the apparent adhesion force by water and thus does not represent the true chemical hydrolysis process.

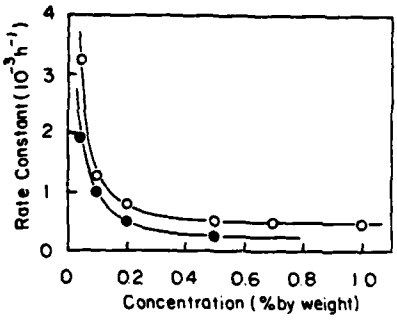

Figure 47. Rate constant of the loss of adhesive strength by hydrothermal degradation for adhesive coating on a glass treated with silane solutions at various concentrations.

o γ-glycidoxypropyltrimethoxysilane
• β-aminoethyl-γ-aminopropyltriethoxysilane

The k' leveled off around 0.5% by weight. It should be noted that silanes were blended in the epoxy rather than the direct treatment on the substrate. Although preferential adsorption of silane molecules on the substrate and existence of a critical silane concentration for effective reinforcement are expected, the role of a blended coupling agent in a matrix is least understood molecularly.

The hydrothermal degradation of interfaces may in some cases appear to improve the impact strength of a composite in sacrifice of the shear strength. According to Broutman et al.,[134] the impact strength showed a minimum at a certain shear strength (Figure 48). Above and below this shear strength, the impact strength increased. In general, the shear strength of glass-fiber reinforced plastics is in the vicinity of the minimum. Thus good adhesion with a proper coupling agent or poor adhesion with a release agent both improve the impact strength. If poor adhesion is chosen to improve impact strength, the hydrothermal degradation of the interface may further improve the impact strength with, of course, decreased shear strength. If overall improvement in mechanical strength in addition to the impact strength is desired, the choice of a proper coupling agent is recommended.

Another important problem is that most glass fibers are multicomponents and often hererogeneous on the surface structure. Thus, the surface is covered with the surface SiOH, AlOH, and other hydroxyl groups of corresponding metal oxides. Silanol groups of a silane are believed to form oxane bonds with

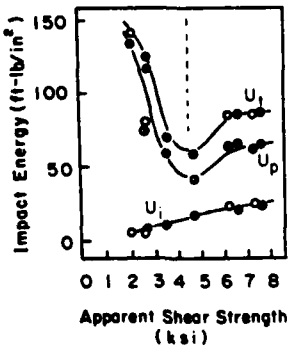

Figure 48. Impact behavior of glass cloth reinforced polyester laminates: Ut, Up, and Ui represent the total impact energy, propagation energy and initiation energy, respectively. (●,ϕ) dry and (o,Φ) wet samples. Effect of water was examined after 7 days immersion in water.

most metal oxides. However, the hydrolytic stability of the various bonds such as SiOSi, SiOAl, SiOTi and other bonds are expected to be different. When the water penetrates to the glass/silane interface, it is possible that water preferentially hydrolyzes the weakest bonds and water collects near the site, since the hydrolysis product acts as a driving force for water penetration. The osmotic pressure created by the collection of water can be fairly high and impose the strain on the surrounding chains making the bond vulnerable to further hydrolytic attack. If this phenomenon takes place, the hydrolytic stability of the interface is lower than that expected from the knowledge based on the siloxane bond.

CONCLUSION

A remarkable advancement has been made in the past several years in the area of molecular and microstructure of composites, coatings and adhesive joints. Especially noteworthy is the improved understanding of the structure of silane coupling agents in aqueous solution as well as on the substrates. Analyses by diversified modern spectroscopic techniques suitable for surface and interface analysis have now become routine.

Specific advancements worth mentioning are the better understanding of the structure of aminosilane, the organization and orientation of silane molecules, structural gradients in the interfacial regions, chemical reactions at the interfaces and within the silane layers, and the structural changes in the

silane layers with the various conditions such as treatment methods, pH of the silane solution, concentration, drying conditions, surface topology and many other factors.

Various new concepts were proposed explaining the reinforcement mechanisms under dry and wet conditions. Importance of interpenetrating networks was stressed along with the formerly believed chemical bonding theory. Actual application examples using non-silane compounds seem to support the idea. Emphasis was also placed on the structure of silane in aqueous solution, which influences the structure of the silane interphase affecting further the mechanical and physical properties of composites, coatings, adhesive joints, and other systems utilizing interfaces. The interfacial structure of coatings can be controlled based on the understandings described in this paper; however, proper recognition of materialistic differences among them is essential.

ACKNOWLEDGMENT

The author wishes to thank the Materials Research Laboratory Program at Case Western Reserve University supported by the MRL Program of the National Science Foundation and the Office of Naval Research for the financial support for this research.

REFERENCES

1. H. Ishida and J.L. Koenig, Polym. Eng. Sci. 18, 128 (1978).
2. E.P. Plueddemann in "Proc. 24th Ann. Tech. Conf., Reinf. Plastics/Composites Div.", SPI, Section 19-A (1969).
3. P.T.K. Shih and J.L. Koenig, Mat. Sci. Eng. 20, 137 (1975).
4. E.P. Plueddemann and G.L. Stark in "Proc. 32nd Ann Tech. Conf., Reinf. Plastics/Composites Div.", SPI, Section 4-C (1977).
5. H.A. Clark and E.P. Plueddemann, Mod. Plast. 40, 133 (1963).
6. H. Ishida and J.L. Koenig, Appl. Spectroscopy 32, 462 (1978).
7. H. Ishida and J.L. Koenig, Appl. Spectroscopy 32, 469 (1978).
8. P.W. Erickson and E.P. Plueddemann in "Interfaces in Polymer Matrix Composites", E.P. Plueddemann, editor, p. 14, in the series of "Composite Materials", L.J. Broutman and R.H. Krock, editors, Academic Press, New York (1974).
9. H. Ishida, C. Chiang, and J.L. Koenig, Polymer, in press.
10. E.P. Plueddemann in "Proc. 25th Ann. Tech Conf., Reinf. Plastics/Composites Div.", SPI, Section 13-D (1970).
11. H. Ishida, S. Naviroj, S.K. Tripathy, J.J. Fitzgerald, and J.L. Koenig, J. Polym. Sci.-Phys., accepted.

12. E.P. Plueddemann in "Silylated Surfaces", Midland Macromolecular Monographs No. 7, D.E. Lyden and W. Collins, editors, p. 38, Gordon and Breach, New York (1980).
13. E.P. Plueddemann, (October 1980), private communication.
14. W.A. Zisman, Ind. Eng. Chem. Product R & D 8, 98 (1969).
15. W.D. Bascom, Macromolecules 5, 792 (1972).
16. R.L. Kaas and J.L. Kardos, Polym. Eng. Sci. 11, 11 (1971).
17. G.D. Nichols, D.M. Hercules, R.C. Peek, and D.J. Vaughan, Appl. Spectroscopy 28, 219 (1974).
18. H.R. Anderson, Jr., F.M. Fowkes, and F.H. Hielscher, J. Polym. Sci.-Phys. 14, 87 (1976).
19. F.J. Boerio and J.E. Greivenkamp in "Proc. 32nd Ann. Tech. Conf., Reinf. Plastics/Composites Div.", SPI, Section 4-A (1977).
20. C.L. Frye, G.E. Vogel, and J.A. Hall, J. Am. Chem. Soc. 83, 996 (1961).
21. C.L. Frye, J. Am. Chem. Soc. 92, 1205 (1970).
22. C.L. Frye, G.A. Vincent, and W.A. Finzel, J. Am. Chem. Soc. 93, 6805 (1971).
23. S.A. Francis and A.H. Ellison, J. Opt. Soc. Am. 49, 131 (1959).
24. R.G. Greenler, J. Chem. Phys. 44, 310 (1966).
25. A.F. Diaz, U. Hetzler, and E. Kay, J. Am. Chem. Soc. 99, 6780 (1977).
26. P.R. Moses, L.M. Wier, J.C. Lennox, H.O. Finklea, J.R. Lenhard, and R.W. Murray, Anal. Chem. 50, 576 (1978).
27. L.H. Lee, J. Colloid Interface Sci. 27, 751 (1968).
28. E.P. Plueddemann, J. Adhesion 2, 184 (1970).
29. H.F. Weetall and L.S. Hersh, Biochim. Biophys. Acta 206, 54 (1970).
30. C.S.P. Sung and S.H. Lee, Polymer Preprint 19, 788 (1978).
31. V.A. Bershtein and V.V. Nikitin, Dokl. Akad. Nauk,. SSSR 190, 832 (1970).
32. V.A. Bershtein, Yu. D. Varfolomev, and V.V. Nikitin, Fiz. Tverd. Tela 13, 693 (1971).
33. C-h Chiang, H. Ishida, and J.L. Koenig, J. Colloid Interface Sci. 74, 396 (1980).
34. F.J. Boerio, S.Y. Cheng, L. Armogan, J.W. Willians, and C. Gosselin in "Proc. 35th Ann. Tech. Conf., Reinf. Plastics/ Composites Div.", SPI, Section 23-C (1980).
35. N.H. Sung and C.S.P. Sung in "Proc. 35th Ann. Tech. Conf., Reinf. Plastics/Composites Div.", SPI, Section 23-B (1980).
36. H. Ishida, unpublished data.
37. F.J. Boerio and J.W. Willians in "Proc. 36th Ann. Tech. Conf., Reinf. Plastics/Composites Div.", SPI, Section 2-F (1981).
38. S. Naviroj, J.L. Koenig, and H. Ishida in "Proc. 37th Ann. Tech. Conf., Reinf. Plastics/Composites Div.", SPI, Section 2-C (1982).
39. N.B. Colthup, L.H. Daly, and S.E. Wiberly, "Introduction to Infrared and Raman Spectroscopy", 2nd edition, p. 415, Academic Press, New York (1975).
40. S. Culler, S. Naviroj, H. Ishida and J.L. Koenig, to be published.

41. H. Ishida and J.L. Koenig, J. Colloid Interface Sci. 64, 555 (1978).
42. H. Ishida and J.L. Koenig, J. Colloid Interface Sci. 64, 565 (1978).
43. M.E. Schrader, I. Lerner, and F.J. D'Oria, Mod. Plast. 45, 195 (1967).
44. O.K. Johannson, F.O. Stark, G.E. Vogel, and R.M. Fleishmann, J. Comp. Materials 1, 278 (1967).
45. H. Ishida S. Naviroj, and J.L. Koenig in "Physicochemical Aspects of Polymer Surfaces", K.L. Mittal, editor, Plenum Publishing, New York, in press.
46. H. Ishida and J.L. Koenig, J. Polym. Sci.-Phys. 17, 1807 (1979).
47. H. Ishida, J.L. Koenig, and K.H. Gardner, J. Chem. Phys., in press.
48. A.T. DiBenedetto and D.A. Scola, J. Colloid Interface Sci. 64, 480 (1978).
49. H. Ishida and J.L. Koenig, J. Polym. Sci.-Phys. 18, 233 (1980).
50. H. Ishida and J.L. Koenig, J. Polym. Sci.-Phys. 18, 1931 (1980).
51. S. Kaplan, H.A. Resing, and J.S. Waugh, J. Chem. Phys. 59, 5681 (1973).
52. E.O. Stejskal, J. Schaefer, J.M. Henis, and M.K. Tripodi, J. Chem. Phys. 61, 2351 (1974).
53. J.J. Fripiat and H.A. Reising, Surface Sci. 47, 661 (1975).
54. J. Schaefer, E.O. Stejskal, and R. Buchdahl, J. Macromol. Sci.-Phys. B13, 665 (1977).
55. D.L. Vanderhart and A.N. Garroway, J. Chem. Phys. 71, 2773 (1979).
56. C-h. Chiang, N-i. Liu, and J.L. Koenig, J. Colloid Interface Sci., in press.
57. D.E. Leyden, D.S. Kendall, L.W. Burggraf, F.J. Pern, and M. DeBello, Anal. Chem., in press.
58. A.D.H. Clague, G.R. Hays, and R. Huis, Koninlkijke/Shell-Laboratorium, Amsterdam, Technical Report 275-17 (1981), and G.R. Hays, A.D.H. Clague, and R. Huis, submitted to Surf. Sci.
59. W. Ritchy and J.L. Koenig, to be published.
60. K. Tanaka, S. Shinoda, and Y. Saito, Chem. Lett. 179 (1979).
61. E.T. Lippma, M.A. Alla, T.J. Pehk, G. Engelhardt, J. Am. Chem. Soc. 100, 1929 (1978).
62. E. Lippma, M. Magi, A. Samoson, G. Engelhardt, and A.R. Grimmer, J. Am. Chem. Soc. 102, 4889 (1980).
63. G.E. Maciel and D.W. Sindorf, J. Am. Chem. Soc. 102, 7606 (1980).
64. D.S. Kendall and D.E. Leyden, to be published.
65. F.J. Boerio and C.A. Gosselin in "Proc. 36th Ann. Tech. Conf., Reinf. Plastics/Composites Div.", SPI, Section 2-G (1981).
66. S. Yoshida and H. Ishida in "Proc. 37th Ann. Tech. Conf., Reinf. Plastics/Composites Div.", SPI, Section 2-F (1982).
67. R.P. Young and N. Sheppard, J. Catal, 7, 223 (1967).
68. R.P. Young and N. Sheppard, Trans. Faraday Soc. 63, 229 (1967).

69. B.J. Fontana and J.R. Thomas, J. Phys. Chem. 65, 480 (1961).
70. M. Gettings and A.J. Kinloch, J. Mat. Sci. 12, 2511 (1977).
71. J.F. Cain and E. Sacher, J. Colloid Interface Sci. 67, 538 (1978).
72. E.P. Plueddemann in "Interfaces in Polymer Matrix Composites", E.P. Plueddemann, editor, in the series of "Composite Materials", L.J. Broutman and R.H. Krock, editors, Academic Press, New York (1974).
73. F.M. Fowkes, J. Adhesion 4, 155 (1972).
74. E.P. Plueddemann, "Silane Coupling Agent", Plenum Press, New York (1982), in press.
75. S. Naviroj, S. Culler, J.L. Koenig, and H. Ishida, Symp. on FT-IR Tech. in Plast. Charact. and Processing, ASTM, submitted.
76. O.K. Johannson, F.O. Stark, and R. Baney, AFML-TRI-65-303, Part I (1965).
77. R. Wong, J. Adhesion 4, 171 (1972).
78. N.H. Sung, A. Kaul, S. Ni, C.S.P. Sung, and I.J. Chin in "Proc. 36th Ann. Tech. Conf., Reinf. Plastics/Composites Div.", SPI, Section 2-B (1981).
79. R.E. Johnson, Jr. and R.H. Dettre in "Surface and Colloid Science", Vol. 2, E. Matijevic, editor, p. 121, Wiley, New York (1969).
80. L. Penn and B. Miller, J. Colloid Interface Sci. 77, 574 (1980).
81. L. Penn and E.R. Bowler, Surface Interface Analy. 3, 161 (1981).
82. H. Hosaka and K. Meguro, Prog. Org. Coat. 2, 315 (1973/74).
83. H. Ishida and J.L. Koenig, J. Polym. Sci.-Phys. 17, 615 (1979).
84. C-h. Chiang and J.L. Koenig in "Proc. 35th Ann. Tech. Conf., Reinf. Plastics/Composites Div.", SPI, Section 23-D (1980).
85. C-h. Chiang and J.L. Koenig in "Proc. 36th Ann. Tech. Conf., Reinf. Plastics/Composites Div.", SPI, Section 2-D (1981).
86. E.P. Plueddemann and G.L. Stark in "Proc. 32nd Ann. Tech. Conf., Reinf. Plastics/Composites Div.", SPI, Section 4-C (1977).
87. A.D. Jonath and J. Crowley in "Adhesion and Adsorption of Polymers, L.H. Lee, editor, Vol. 12A, p. 175, Plenum Press, New York (1980).
88. G.C. Knollman, J.J. Hartog, and A.D. Jonath, to be published.
89. Yu. S. Lipatov and F.G. Fabulyak, Vysokomol. Soed. 11, 708 (1969).
90. Ye. B. Trotyanskaya, A.M. Poimanov, and Ye. F. Nosov, Vysokomol. Soed. 15, 612 (1973).
91. V.P. Gordienko and V.P. Solomko, Vysokomol. Soed. 12, 399 (1970).
92. Ye. G. Moisya, G.M. Semenovich, and Ye. S. Lipatov, Vysokomol. Soed. 15, 1337 (1973).
93. L.D. Tryson and J.L. Kardos in "Proc. 36th Ann. Tech. Conf., Reinf. Plastics/Composites Div.", SPI, Section 2-E (1981).

94. L.T. Drzal, M.J. Rich, and P.J. Lloyd, Polymer Preprints 22, 199 (1981).
95. G.N. Savin, "Stress Concentration Around Holes", p. 234, Pergamon Press, London (1961).
96. J. Delmonte, "Technology of Carbon and Graphite Fiber Composites", Van Nostrand, New York (1981).
97. L.T. Drzal, J.A. Mesher, and D.L. Hall, AFWAL-TR-80-4030 (1980).
98. L.T. Drzal, M.J. Rich, J.D. Camping, and W.J. Park, AFWAL-TR-81-4003 (1981).
99. L.T. Drzal and G.E. Hammer, AFWAL-TR-80-4143 (1981).
100. A. Kelly and W.R. Tryson, J. Mech. Phys. Solids 13, 329 (1965).
101. A.T. DiBenedetto and D.A. Scola, J. Colloid Interface Sci. 74, 150 (1980).
102. P.W. Erickson, A.A. Volpe, and E.R. Cooper in "Proc. 19th Ann. Tech. Conf., Reinf. Plastics/Composites Div.", SPI, Section 21-A (1964).
103. F.J. Mayer and S. Newman in "Proc. 34th Ann. Tech. Conf., Reinf. Plastics/Composites Div.", SPI, Section 14-G (1979).
104. E.P. Plueddemann and G.L. Stark in "Proc. 35th Ann. Tech. Conf., Reinf. Plastics/Composites Div.", SPI, Section 20-B (1980).
105. C.M. Balik and A.J. Hopfinger, Macromolecules 13, 999 (1980).
106. S.E. Rickert and E. Baer, J. Mat. Sci. 13, 451 (1978).
107. S.E. Rickert, E. Baer, J.C. Wittmann, and A.J. Kovacs, J. Polym. Sci.-Phys. 16, 895 (1978).
108. D.R. Stevenson, O.M. Windrath, and D.R. Burge, Plast. Compound, July/August, 47 (1981).
109. T. Nakatsuka, H. Kawasaki, K. Itadani, and S. Yamashita, J. Appl. Polym. Sci. 24, 1985 (1979).
110. P. Dreyfuss, Macromolecules 11, 1031 (1978).
111. P. Dreyfuss, L.J. Fetters, and A.N. Gent, Macromolecules 11, 1036 (1978).
112. M.R. Rosen and E.D. Goddard in "Proc. 34th Ann. Tech. Conf., Reinf. Plastics/Composites Div.", SPI, Section 19-E (1979).
113. R.D. Kilkarni and E.D. Goddard in "Proc. 35th Ann. Tech Conf., Reinf. Plastics/Composites Div.", SPI, Section 20-E (1980).
114. S.J. Monte and G. Sugerman in "Proc. 31st Ann. Tech. Conf., Reinf. Plastics/Composites Div.", SPI, Section 6-E (1976).
115. S.J. Monte and G. Sugerman in "Proc. 32nd Ann. Tech. Conf., Reinf. Plastics/Composites Div.", SPI, Section 4-E (1977).
116. S.J. Monte and G. Sugerman in "Proc. 33rd Ann. Tech. Conf., Reinf. Plastics/Composites Div.", SPI, Section 2-B (1978).
117. S.J. Monte and G. Sugerman in "Proc. 34th Ann. Tech. Conf., Reinf. Plastics/Composites Div.", SPI, Section 16-E (1979).
118. S.J. Monte and G. Sugerman in "Proc. 35th Ann. Tech. Conf., Reinf. Plastics/Composites Div.", SPI, Section 23-F (1980).
119. S.J. Monte and G. Sugerman in "Proc. 36th Ann. Tech. Conf., Reinf. Plastics/Composites Div.", SPI, Section 18-D (1981).

120. C.D. Han, C. Sandford, and H.J. Yoo, Polym. Eng. Sci. 18, 849 (1978).
121. C.D. Han, T. van den Weghe, P. Shete, and J.R. Haw, Polym. Eng. Sci. 21, 196 (1981).
122. Y-g. Kim and H-y. Fan, Plastics (People's Rep. China) 3, 1 (1981).
123. Y-g. Kim and H-y. Fan, Plastics (People's Rep. China) 3, 18 (1981).
124. Y-g. Kim and H-y. Fan, Plastics (People's Rep. China) 4, (1981).
125. H. Ishida, J.L. Koenig, B. Asumoto, and M.E. Kenney, Polym. Comp. 2, 75 (1981).
126. B. Arkles and W. Peterson in "Proc. 35th Ann. Tech. Conf., Reinf. Plastics/Composites Div.", SPI, Section 20-A (1980).
127. N.K. Eib, K.L. Mittal, and A. Friedrichs, J. Appl. Polym. Sci. 25, 2435 (1980).
128. M. Kokubo, H. Inagawa, M. Kawahara, D. Terunuma, and H. Nohira, Kubunshi Ronbunshu 38, 201 (1981).
129. E.P. Plueddemann, J. Paint Technol. 10, 1 (1968).
130. N.K. Eib, K.L. Mittal, and H.R. Anderson, Jr. in "Proc. of 54th Colloid and Surface Sci.", ACS, Lehigh University, Bethlehem, Pa., June 1980.
131. E.H. Andrews, H.P. Sheng, M.A. Majid, and C. Vlachos in "Proc. of the Techniques for the Characterization of Composite Materials", sponsored by ONR, M.I.T., Cambridge, Massachusetts, June 1981.
132. E.H. Andrews and A. Stevenson, J. Mat. Sci. 13, 1680 (1978).
133. E.H. Andrews and A. Stevenson, J. Adhesion 11, 17 (1980).
134. P. Yeung and L.J. Broutman in "Proc. 32nd Ann. Tech. Conf., Reinf. Plastics/Composites Div.", SPI, Section 9-B (1977).